Selective harmonic elimination in PUC-5 multilevel inverter using hybrid IGWO-DE and Honey Badger algorithm

Final report phase 1

Submitted By

Mohd Anas Khan	**Zaid Sifat**	**Muaadh AbdulHakim**	**Prabhat Kumar**
GJ1936	GI7258	GK3945	GK9199
18EEB166	18EEB512	17EEB189	18EEB30

Under the supervision of Dr Adil Sarwar

Department of electrical engineering, AMU

CANDIDATE'S DECLARATION

We hereby certify that the work which is being presented in the project entitled "**Selective harmonic elimination in PUC-5 multilevel inverter using novel hybrid IGWO-DE and Honey Badger Algorithm**" in partial fulfilment of the requirements for the award of the Degree of Bachelor of Technology and submitted in the Department of Electrical Engineering, Zakir Hussain College of Engineering and Technology of the Aligarh Muslim University, Aligarh is an authentic record of our work carried out during a period from August, 2021 to April, 2022 under the supervision of **Dr Adil Sarwar**, Assistant Professor, Department of Electrical Engineering, Z.H.C.E.T, Aligarh Muslim University, Aligarh, India.

The matter presented in this project has not been submitted by us for the award of any other degree of this or any other Institute.

Mohd Anas Khan	**Zaid Sifat**	**Muaadh AbdulHakim**	**Prabhat Kumar**
GJ1936	GI7258	GK3945	GK9199
18EEB166	18EEB512	17EEB189	18EEB30

This is to certify that the above statement made by the candidates is correct to the best of my knowledge.

Dr. Adil Sarwar

(Supervisor)

TABLE OF CONTENTS

Page No

List of Figures

CHAPTER 1

1.INTRODUCTION

1.1 Brief Overview of Multilevel Inverter

The demand for a multilevel inverter is growing every day because it has numerous applications in high-power applications such as electric vehicles [1], electric drives[2], flexible AC transmission systems, laminators, mills, and conveyors, and most importantly, it plays an important role in power conversion from renewable energy sources [3][4][5]. The advantages provided by MLI, such as generating a step wise output waveform that reduces harmonic content, lower stress across semiconductor devices, etc., are the reason for many pf applications of MLI. In spite of several advantages, power electronics converters are facing the problem of harmonics. These harmonics have detrimental effects on certain applications e.g., degrade efficiency, produce torque pulsation in the electrical drives and reduce the lifespan of the system. Researchers have developed various control and modulation techniques in order to reduce harmonics and increase the efficiency and performance of power electronics converters. Due to its tight control over harmonic spectrum in the voltage produced by power electronics converters, selective harmonic elimination technique is widely adopted by various researchers. Selective harmonic elimination (SHE)[6] has been a widely researched alternative to traditional modulation techniques. It has been researched that SHE has many advantages over other traditional modulation techniques such as acceptable performance with low switching frequency to fundamental frequency ratios, direct control over output waveform harmonics[7]. These are the benefits which make SHE an appropriate alternative to various applications including variable speed drives, ground power units. The concept of SHE is basically based on Fourier series decomposition of voltage waveform produced by power electronics converters and calculating optimized switching angles in order to reduce unwanted lower order harmonics. The idea is basically to set the lower order harmonics to zero and maintain the fundamental component at a predefined value. For this purpose, complex nonlinear transcendental equations are solved for finding optimized switching angles. SHEPWM has various approaches to get these optimized switching angles and can be categorized as 1) Numerical methods (NMs) 2) Algebraic methods (AMs) and 3) Evolutionary algorithms (EAs).

1.2 Overview of Metaheuristic Techniques

Numerical methods are iterative techniques that find the best solution iteratively by guessing the best initial solution. Numerous numerical approaches for solving the SHEPWM transcendental equations have been published in the literature, including the Newton Raphson method[8] and the Gauss Newton method [9][10]. However, guessing the correct initial solution remains a difficult process, and there is no established approach for determining the optimal solution[11]. Algebraic techniques were introduced to address the issue of initial guessing with numerical methods[11]. These methods do not involve guessing the initial solutions and solve transcendental equations after transforming them to polynomial equations and then solved to find switching angles for minimizing the THD[12]. Many strategies have been proposed in the literature for solving these polynomial equations, such as Resultant theory[13], which converts the polynomial equation into equivalent triangular form, which may then be solved in the same manner as Gaussian elimination is used to solve linear equations. For improving the efficiency of Algebraic method many other methods including Groebner Bases Theory[12], Symmetric polynomial theory[14] and the power sum[15] were introduced in the literature. Although algebraic methods can find global optima, they require an advanced microprocessor to convert non-linear or transcendental equations into high degree polynomial equations, and the degree increases with the level of power electronic converters, increasing the computational burden and requiring a large amount of memory in a microprocessor, which ultimately leads to an increase in cost[16][11][7]. Evolutionary algorithms, also known as heuristic techniques, are used to find optimum switching angles for removing lower order harmonics and minimizing THD. Furthermore, these techniques are simple in structure and require less computational power from the processor, as well as being less reliant on a suitable initial guess[7]. Many evolutionary algorithms have been described in the literature, including the Genetic Algorithm (GA)[17], the Differential Evolution (DE)[18], Bee Algorithm (BA)[19], the Colonial Competitive Algorithm (CCA)[20], Generalized Pattern Search (GPS)[21], Particle Swarm Optimization (PSO)[22], Grey Wolf Optimization (GWO)[23], and many others. However, many of these algorithms suffer from a problem of sticking in local optima, which worsens as the number of transcendental equations increases, making it difficult for algorithms to find feasible solutions. To make a proper balance between exploration and exploitation ability of algorithms many hybrid algorithms like [16][24] [25] are proposed.

1.3 Overview of proposed Algorithm

In this paper a new and improved hybrid algorithm is proposed using two evolutionary algorithm that is Grey wolf optimization with a new and improved convergence factor based on sigmoid function that enhance the searching ability and convergence speed of GWO and Differential evolution with a dynamic scaling factor whose value is higher at initial stages which prevents algorithm to fall into local optima whereas at final stages the value of scaling factor is reduced and enhance the speed of algorithm. And the given IGWO-DE algorithm is used to eliminate the lower order harmonic and to minimize the THD from the output waveform of PUC-5 multilevel inverter topology [26] by solving the transcendental equation generated by the SHEPWM method.

CHAPTER 2

2.LITERATURE REVIEW

2.1 Cascaded H-Bridge Multi-level Inverter

2.1.1 Overview of Cascaded H-Bridge Multi-level Inverter

Cascaded H-Bridge (CHB) multilevel inverter (MLI) is popular and a simpler method of multilevel inverter. Pulse width modulation techniques and high switching frequency are required to generate high-quality output current and voltage waveforms with little ripple. Several H-Bridges are connected in series in a cascaded H-Bridge multilevel inverter. Each H-Bridge has its own DC source, DC sources are often derived using multi-pulse diode rectifiers with phase-shifting transformers to achieve minimal line-current harmonic distortion and a higher input power factor. The benefit of this technology is that no diode or capacitor is required for clamping, and the waveform output is sinusoidal in nature even if the number of levels is increased without filtering.

The main idea behind a MLI is to generate AC waveforms from small voltage steps, The small-voltage steps produce waveforms with lower harmonic distortion and dv/dt. A CHB-MLI can theoretically produce an unlimited number of output voltage levels, when the number of voltage levels is increased the output voltage waveform is extremely similar to a sinusoidal form without an output filter, that has less harmonic distortion, there is two methods to increase the voltage level in CHB. One method is to increase the number of H-bridge cells in the cascade. In this situation, the number of switching devices, diodes, gate amplifiers, and other passive elements is increased, resulting in a reduction in system dependability and stability due to device failure. Another method is the use of asymmetrical dc sources. The number of voltage levels can be raised with asymmetrical dc voltages without raising the number of H-bridge cells.

Full bridge inverter shown in Fig.1, One full-bridge is a three-level CHB-MLI, and each module added in cascade adds two voltage levels to the inverter. A full-bridge inverter is capable of producing three voltages + V_{DC} , - V_{DC} and 0. To adjust one level of voltage in CHB-MLI, one switch in one full-bridge inverter is turned ON and the other switch is turned OFF. To generate a voltage of +Vdc, Switches S_1,as well as S_2, are turned on. To generate a voltage of -Vdc, Switches S_3,as well as S_4 are turned off. When no current flows across the full-bridge this will happen when Switches S_1 and S_3 or S_2 and S_4 are turned on, hence the voltage level drops to zero. Each bridge's output voltage is the total of each cell's voltage. The number of output voltage levels given by 2n + 1, where n is the cells number. Other topologies can only provide half of the overall DC-bus voltage source magnitude, however the CHB-MLI can produce the total voltage source value for both positive half cycle and negative half cycle.

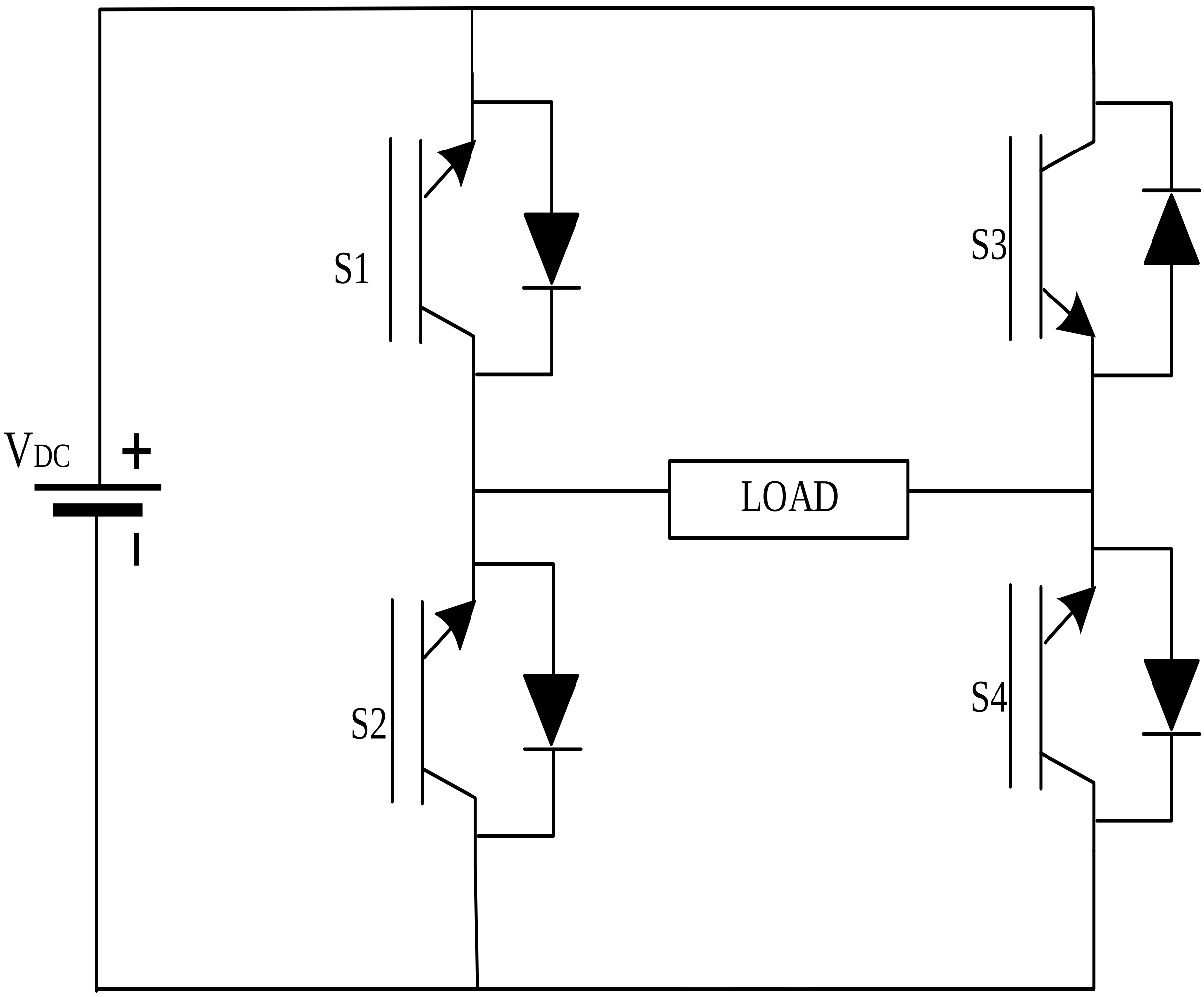

Figure 1: CHB multilevel inverter

Following equation describe the number of required components for CHB-MLI:

1- No. of main switches = 2(N-1), where N = number of levels
2- No. of diodes = 2(N-1)

Number of switches: [1]

1- Four switches are required for a 3 -level CHB multilevel inverter.
2- Eight switches are required for a 5 -level CHB multilevel inverter.
3- Twelve switches are required for a 7-level CHB multilevel inverter.
For more than 7 level inverter we can use following formula [2]:

No. of Switches = 2(N-1), where N = number of levels

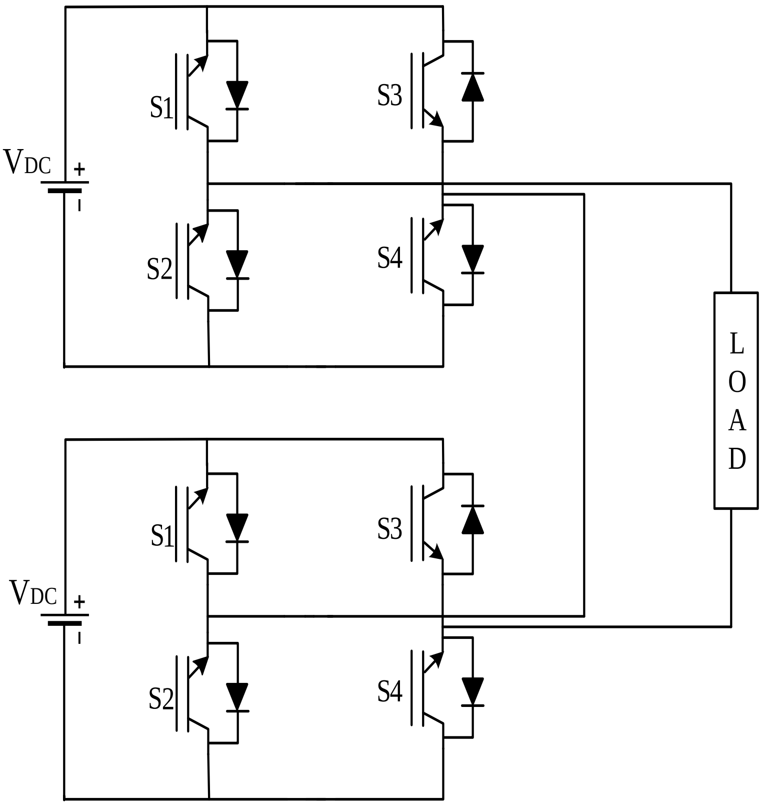

Figure 2: CHB-5 multilevel inverter

Two full-bridge inverters are linked in series in Fig. 2 to produce five different output voltage levels +2V_{dc}, +V_{dc}, 0 V_{dc}, - V_{dc} and - 2V_{dc}. The benefits of this sort of MLI are that it requires fewer components than flying capacitor or diode clamped inverters.

2.1.2 Operation Modes of Five Level Cascaded H-Bridge Multi-level Inverter

Mode1 (+2V_{dc}): The operating mode for obtaining a +2V_{dc} output voltage is shown in (Fig.3). Switches SW_1, SW_2, SW_5, and SW_6 are on in this mode, whereas switches SW_3, SW_4, SW_7, and $SW_8$are off.

Mode2 (+V_{dc}): The operating mode for obtaining a +V_{dc} output voltage is shown in (Fig.4). Switches SW_1, SW_2, SW_6, and SW_8 are on in this mode, whereas switches SW_3, SW_4, SW_5, and $SW_7$are off.

Mode3 (0): The operating mode for obtaining a zero-output voltage is shown in (Fig. 5). There will be no current flow in the power circuit because the lower-leg switches are triggered.

Mode4 (- 2V_{dc}) : The operating mode for obtaining a -2V_{dc} output voltage is shown in (Fig.6). Switches SW_3, SW_4, SW_6, and SW_8 are on in this mode, whereas switches SW_1, SW_2, SW_5, and SW_7 are off. The direction of current flow in the opposite direction of load current.

Mode5 (- V_{dc}): The operating mode for obtaining a -V_{dc} output voltage is shown in (Fig.7). Switches SW_3, SW_4, SW_7, and SW_8 are on in this mode, whereas switches SW_1, SW_2, SW_5, and $SW_6$are off. The direction of current flow in the opposite direction of load current.

2.2 Packed U Cell Multi-level Inverter:

2.2.1 Overview of PUC Multi-level Inverter

Multilevel inverter provides multilevel output voltage waveform. They generate desired output voltage from several DC voltage level at its input. Earlier, two level inverter were most commonly used which provided two different voltages for the load i.e. suppose we are providing V as an input to a two level inverter then it will provide + V/2 and – V/2 on output. Although this method was effective but it provided only two step output and it creates problems specifically where high distortion in the output voltage is not required. With advancement in technology MLI (Multi level inverter) were invented which gave multi step desired output with very less harmonic distortion. There are lots of multilevel inverter topologies was given in literature such as cascaded H bridge (CHB)[27], Flying capacitor(FC)[28], neutral point clamped(NPC)[29], diode clamped[30] etc. All the multilevel inverter mentioned above has a shortcoming that it requires a large number of DC sources and switches which results in higher cost and complicated implementation. In order to overcome the issues related to conventional multilevel inverter pack U cell topology [26][31][32] which requires less number of switches and only one DC source. However, CHB required (L-1)/2 sources for L level inverter. Furthermore, it requires only half of the Dc sources and one third of capacitors compared with FC. PUC inverter for a five level inverter in which six switches, one DC source and a capacitor act as a second source as shown in Figure 3:

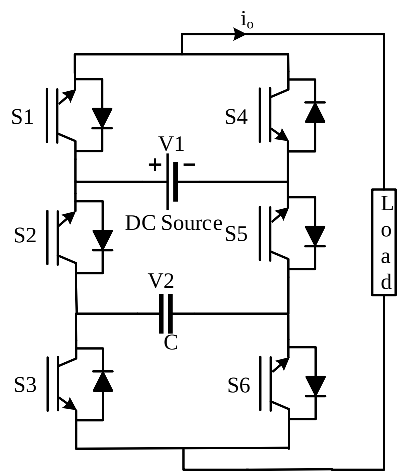

Figure 3: PUC-5 multilevel inverter

2.2.2 Operation Modes of Five Level PUC Multi-level Inverter:

In this type of topology (S1&S6), (S2&S5), (S3&S4) cannot conduct at a same time or simultaneously so there are only three switches for which we need to give pulses and for remaining three we can give complementary pulses. For this type of inverter there are only eight possible states for conduction as shown in the switching table of PUC inverter given in Table 1. The sequence of the operation of the converter describing the eight possible states is therefore given in Figure 4. For generating five level output waveform consider V1 = 2E and V2 = E so 2E, + -E, 0 are the 5 levels of output waveform [32]. From the table it can be concluded that it have redundant switching states which is necessary for an easy voltage balancing without adding any external controllers for controlling the voltage across capacitors.

Table 1 : Switching Table of PUC-5 multilevel inverter

States	S1	S2	S3	Output Voltage	Effect on Capacitor
1	1	0	0	V1	No effect
2	1	0	1	V1-V2	Charging
3	1	1	0	V2	Discharging
4	1	1	1	0	No Effect
5	0	0	0	0	No Effect
6	0	0	1	-V2	Discharging
7	0	1	0	(V1–V2)	Charging
8	0	1	1	-V1	No effect

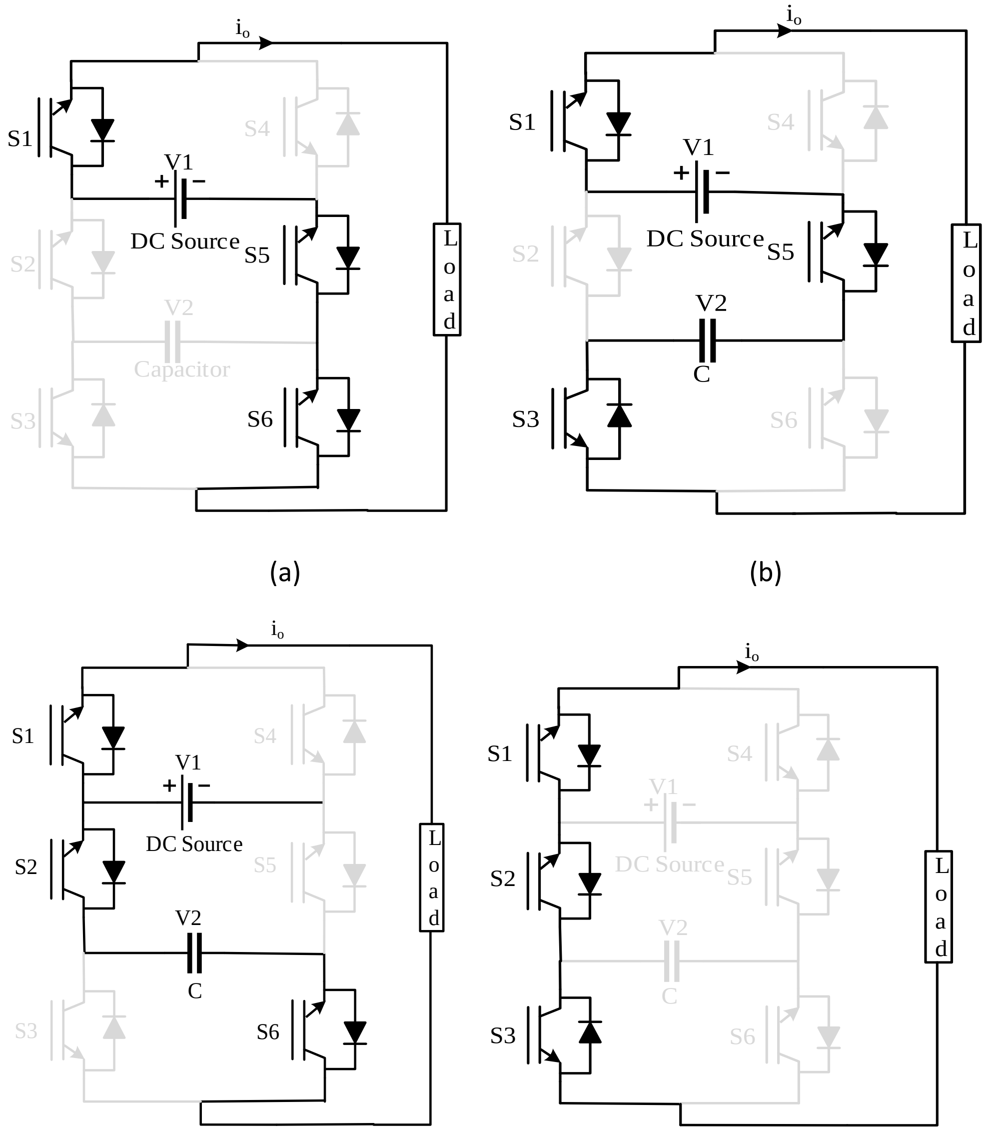

(a) (b)

(c) (d)

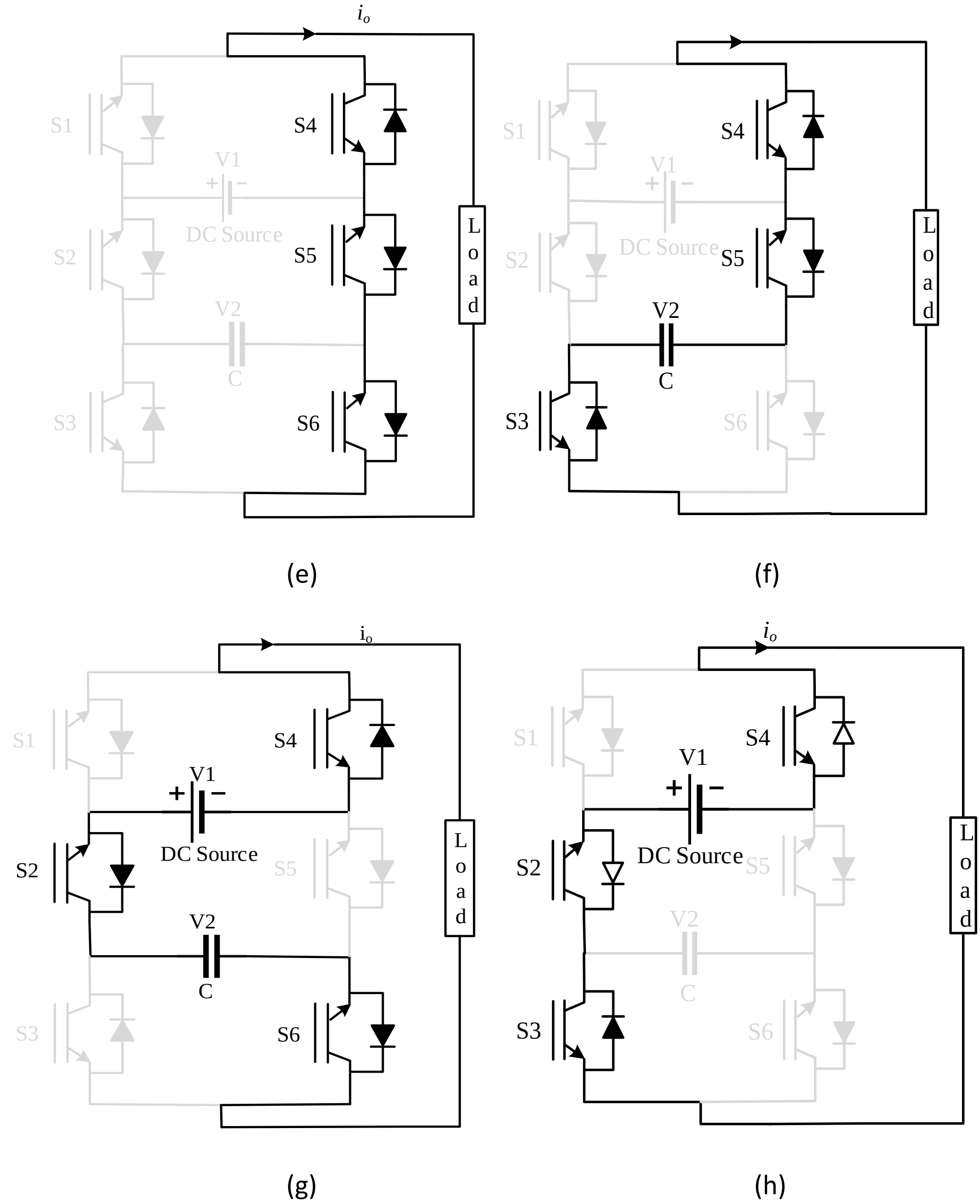

Figure 4: Switching states of PUC-5 multilevel inverter : (a)=state :1 (b)=state:2 (c)=state:3 (d)=state:4 (e)=state:5 (f)=state:6 (g)=state:7 (h)=state:8

2.3 Selective Harmonic Elimination (SHE):

To reduce total harmonic distortion (THD), a variety of pulse width modulation techniques have been reported in the literature, including sinusoidal PWM (SPWM), space vector PWM, selective harmonic mitigation (SHMPWM)[33], selective harmonic elimination (SHE-PWM), and many others. The SHE-PWM and SHM-PWM techniques are the most popular among these PWM techniques. In the SHM-PWM technique, we minimise the low order harmonics, whereas in the SHE-PWM technique, we totally eliminate some of the low order harmonics, lowering the THD and using fewer non-linear equations to obtain the firing angles. To determine the switching angle values, namely ($\alpha_1, \alpha_2, \alpha_3 \ldots\ldots \alpha_s$), in order to eliminate $(s-1)$ odd harmonics, consider the fourier series of the output voltage signal of the PUC-5 multilevel inverter with quarter wave symmetry, as shown in Figure 5:

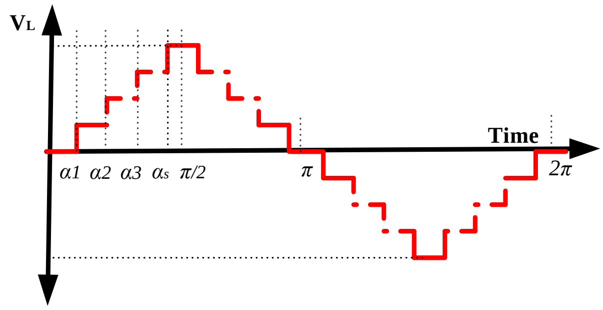

Figure 5: Output Voltage waveform of PUC Inverter topology

Since the output voltage has a quarter wave symmetry, it contains only odd harmonic so $a_0 = 0$ and $a_n = 0$ and the fourier series of output voltage will be:

$$V_o(\omega t) = a_0 + \sum_{n=1}^{\infty} a_n \cos(n\omega t) + \; b_n \sin\,(n\omega t)$$

$$V_O(\omega t) = \sum_{n=1}^{\infty} V_n \sin(n\omega t)$$

Where V_n is the nth harmonic given by :

$$V_n = \begin{cases} \dfrac{4V_{dc}}{n\pi} \displaystyle\sum_{k=1}^{s} \cos\,(n\alpha_k), & n = odd \\ 0 & n = even \end{cases}$$

Where V_{dc} is the nominal DC voltage, *n* is the odd harmonic order, *s* is the number of switching angle given by *(L-1)/2* and α_k is the switching angles in the order $(0 < \alpha_1 < \alpha_2 < \alpha_3 \ldots \ldots . < \alpha_k < 90)$. The fundamental component voltage is given by:

$$\frac{4V_{dc}}{\pi}[\cos(\alpha_1) + \cos(\alpha_2) \ldots \ldots \ldots + \cos(\alpha_s)] = \; V_1$$

$$\cos(\alpha_1) + \cos(\alpha_2) \ldots \ldots \ldots + \cos(\alpha_s) = sM\frac{\pi}{4}$$

Where *M* is the modulation index ranges from 0 to 1.1. In SHE *s* that is degree of freedom in which one degree of freedom is used to control the magnitude of fundamental component and remaining (*s*-1) degree of freedom are used to eliminate the n^{th} order harmonic as they dominate on THD so the transcendental equation that we have to solve are as follows:

$$\mathrm{Cos}(\alpha_1) + \cos(\alpha_2) \ldots \ldots \ldots + \cos(\alpha_s) = Ms\frac{\pi}{4}$$

$$\cos(3\alpha_1) + \cos(3\alpha_2) \ldots \ldots \ldots + \cos(3\alpha_s) = 0$$

$$\cos(5\alpha_1) + \cos(5\alpha_2) \ldots \ldots \ldots + \cos(5\alpha_s) = 0$$

$$\cos((2S-1)\alpha_1) + \cos((2S-1)\alpha_2) \ldots \ldots \ldots + \cos((2S-1)\alpha_s) = 0$$

In this paper, selective harmonic elimination technique is employed for a 5-level cascaded H-bridge multilevel inverter. So, S= (5-1)/2= 2 means there is a need to solve only two transcendental equation for finding alpha1 and alpha2 for eliminating 3rd harmonic component present in output waveform .

$$\mathrm{Cos}(\alpha_1) + \cos(\alpha_2) \ldots \ldots \ldots + \cos(\alpha_s) = M\frac{\pi}{2}$$

$$\cos(3\alpha_1) + \cos(3\alpha_2) \ldots \ldots \ldots + \cos(3\alpha_s) = 0$$

For solving these equations IGWO-DE technique is used.

2.4 Overview of GWO technique:

Swarm intelligent algorithms are algorithms in which the hunting patterns of animals and birds are mathematically modelled to find global maxima and minima for optimization problems. The GWO algorithm is one of the SI algorithms proposed by Syed Mirjalili in 2014 [34]. Basically GWO algorithm is modelled by taking inspiration from the Grey wolves. The grey wolves are the top predator in the food chain it is because they lived in pack and have a serious social dominant hierarchy among them. Social hierarchy of grey wolves is given in Figure 4. The alpha wolf is the leader wolf who is responsible for taking important decisions and has the greatest knowledge of prey in the peck and the beta wolves helps alpha wolves in taking decision. After alpha, beta, delta wolves comes at third level and has mainly scouts, elders, hunter etc and lastly the omega wolves who just follows the alpha, beta and delta wolves. Similarly, the fittest solution is considered as alpha solution. The beta and delta solution are similar to the second, third optimal solution.

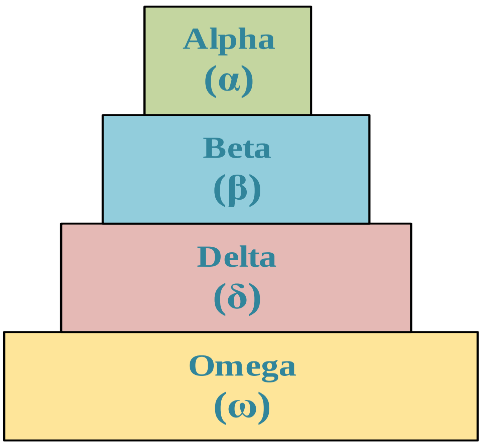

Figure 6: Social hierarchy of grey wolves

Grey wolves have an ability to catch their prey in groups and encircle them while hunting. Mirjaali suggested the following equation to mathematically model the encircling behaviour:

$$\vec{D} = \left|\vec{C}.\overrightarrow{X_p}(t) - \vec{X}(t)\right| \qquad (1)$$

$$\vec{X}(t+1) = \overrightarrow{X_p}(t) - \vec{A}.\vec{D} \qquad (2)$$

Where t denotes the t-th iteration, $\vec{A}$ and $\vec{C}$ represent the coefficient vectors, $\overrightarrow{X_p}$ depicts the prey's location vector, and $\vec{X}$ represents the grey wolf's position vector

The following equation can be used to evaluate the vectors A and C :

$$\vec{A} = 2a.\overrightarrow{r_1} - a \qquad (3)$$

$$\vec{C} = 2.\overrightarrow{r_2} \qquad (4)$$

Where $\overrightarrow{r_1}$, $\overrightarrow{r_2}$ are the random vectors in [0,1] and $\vec{a}$ is a vector that decrease from 2 to 0 as we increase the no of iteration and it can be calculated as follows :

$$a = 2 - 2t/t_{max} \qquad (5)$$

Where t and t_{max} are the current iteration, and maximum number of iteration respectively. The wolf (solution) deviates from its path and searches in a new direction if $|\vec{A}| > 1$ and converge towards the prey (optimum solution) if $|\vec{A}| < 1$, and $\vec{A}$ is a random vector in the interval$[-2a, 2a]$ where a decreases from 2 to 0 over the course of iteration. When the value of $\vec{C}$ is greater than one, the $\vec{C}$ vector often favours exploration, and when the value of $\vec{C}$ is less than one, it favours exploitation. $\vec{C}$ is not linearly decreased in contrast to $\vec{A}$, so this parameter is very useful to avoid the local optima stagnation, particularly in the final iteration.

Grey wolves have an ability to memorize the position of prey and as apha wolves are the leader in the peck so they have a greatest knowledge of prey as to modelled the hunting behaviour of wolves the three best optimal solutions are considered as alpha, beta and delta solution and the remaining omega solutions update their position based on alpha, beta and delta’s position the following equations describes the how the omega solutions are update their position.

$$\overrightarrow{D_\alpha} = \left|\overrightarrow{C_1}.\overrightarrow{X_\alpha} - \vec{X}\right| \qquad (6)$$

$$\overrightarrow{X_1} = \overrightarrow{X_\alpha} - \overrightarrow{A_1}.(\overrightarrow{D_\alpha}) \qquad (7)$$

$$\overrightarrow{D_\beta} = \left|\overrightarrow{C_2}.\overrightarrow{X_\beta} - \vec{X}\right| \qquad (8)$$

$$\overrightarrow{X_2} = \overrightarrow{X_\beta} - \overrightarrow{A_2}.(\overrightarrow{D_\beta}) \qquad (9)$$

$$\overrightarrow{D_\delta} = \left|\overrightarrow{C_3}.\overrightarrow{X_\delta} - \vec{X}\right| \qquad (10)$$

$$\overrightarrow{X_3} = \overrightarrow{X_\delta} - \overrightarrow{A_3}.(\overrightarrow{D_\delta}) \qquad (11)$$

$$\vec{X}(t+1) = \frac{\overrightarrow{X_1} + \overrightarrow{X_2} + \overrightarrow{X_3}}{3} \qquad (12)$$

Where $\overrightarrow{X_\alpha}$, $\overrightarrow{X_\beta}$, $\overrightarrow{X_\delta}$ and $\vec{X}$ are the positions vectors of alpha, beta, delta and the current solution respectively and $\vec{X}(t+1)$ is the final position vector of current solution for next iteration.

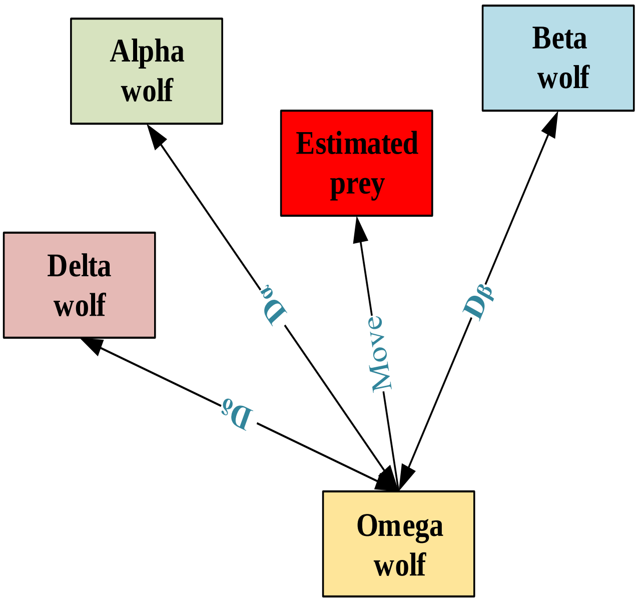

Figure 7: Position updating in GWO

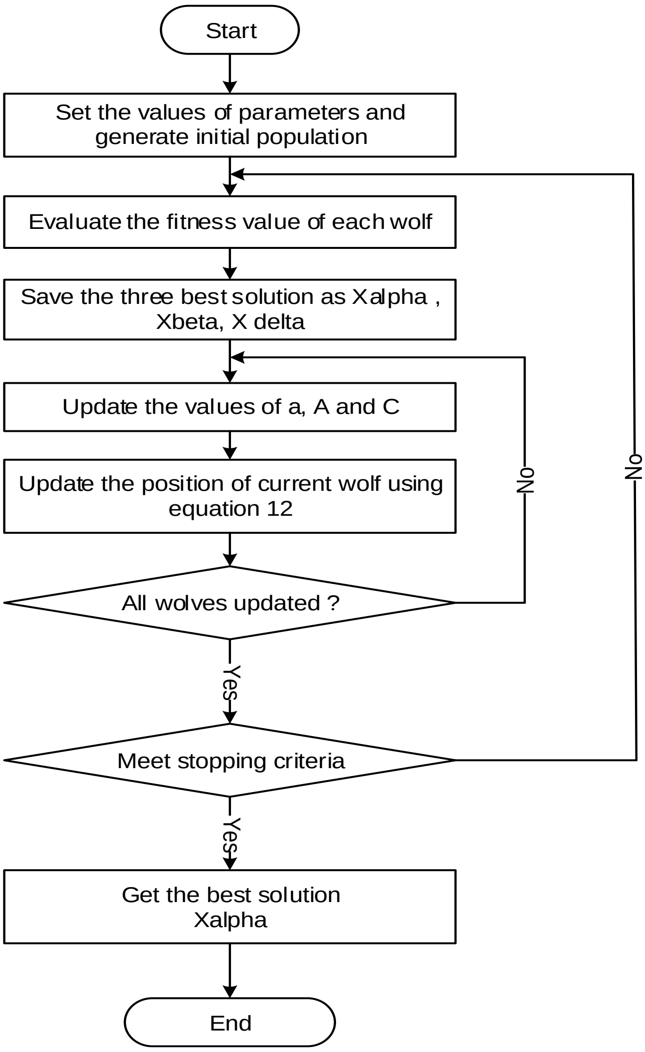

Figure 8: Flowchart of GWO

2.5 Overview of Differential evolution:

Differential evolution[35] is a stochastically population based technique introduced by Storn and Price in 1997. DE belongs to the family of genetic algorithm (GA). DE performs just like a GA and it has following operation: Initialisation, Mutation, Crossover and selection.

2.5.1 Initialization:

DE initialises by considering $\vec{X}_i^t = [x_{i,1}^t,\ x_{i,2}^t,\ x_{i,3}^t \ldots\ldots, x_{i,d}^t\ ]$ be the target vector or initial vector of population size N_p with vector dimension d chosen randomly to cover the entire search space.

2.5.2 Mutation:

The target vector generated from initialisation undergoes mutation to generate the mutant vector $\vec{V}_i^t = [v_{i,1}^t, v_{i,2}^t, v_{i,3}^t, \ldots \ldots, v_{i,d}^t]$ using different mutation strategies such as DE/rand/1, DE/best/1, DE/rand/2, DE/best/2 and many more. In DE/best/1 strategy Among the various mutation strategy DE/rand/1, is the most basic mutation strategy which can be described as follows:

$$\vec{V}_i^t = \vec{X}_{best}^t + F * (\vec{X}_{R2}^t - \vec{X}_{R3}^t) \qquad (13)$$

Where $\vec{X}_{best}^t$ is the best candidate solution as far. R_1, R_2 are randomly chosen indices from $[1,2,3, \ldots., N_p]$ such that $R_1 \neq R_2 \neq i$. And F is the scaling factor ranges from 0 to 1.

2.5.3 Crossover:

The trial vector $\vec{U}_i^t = [u_{i,1}^t, u_{i,2}^t, u_{i,3}^t, \ldots\ldots u_{i,d}^t]$ is generated by recombining the target vector $\vec{X}_i^t$ and mutant vector $\vec{V}_i^t$ through crossover operator. Basically crossover operators are of two type the binomial and exponential crossover operator. The binomial crossover can be described as follows :

$$U_{i,j}^t = \begin{cases} V_{i,j}^t, if\ rand(0,1) \leq CR\ OR\ j = \delta \\ X_{i,j}^t, if\ rand(0,1) > CR\ AND\ j \neq \delta \end{cases} \qquad (15)$$

Where δ is the randomly selected variable location such that $\delta \epsilon \{1,2,3, \ldots\ldots, d\ \}$ to ensure that at least one variable is obtained from the donor vector and CR, the crossover rate or crossover probability which is generally kept high ranges from 0 to 1.

2.5.4 Selection:

In order to know which vector got selected for next iteration between trial vector and target vector, selection operator is used. There are lot's of selection operators such as tournament selection, rank based selection, fitness proportional selection, greedy selection etc. The greedy selection for minimization problem is described as follows:

$$\vec{X}_i^{t+1} = \begin{cases} \vec{U}_i^t, & if\ f(\vec{U}_i^t) \leq f(\vec{X}_i^t) \\ \vec{X}_i^t, & if\ f(\vec{U}_i^t) > f(\vec{X}_i^t) \end{cases} \qquad (16)$$

Where f is the fitness function, $\vec{X}_i^{t+1}$ is the target vector for next generation or iteration. The above expression shows that if the value.

CHAPTER 3

3.PROPOSED ALGORITHM

3.1 The Algorithmic Description:

GWO's searching ability is based on two principles : exploration and exploitation. Exploration refers to the process of exploring new areas or mathematically, the process of looking for a solution as much as possible in a search space in order to prevent local optimum stagnation. On the other hand exploitation refers to looking in the same direction in greater depth or mathematically, searching for a solution with high precision. Using the GWO algorithm to find the global optimum with high efficiency necessitates achieving the proper balance between exploration and exploitation. These two abilities are governed by two parameters, A and C, as described in section 2. As compared to other swarm intelligent techniques, GWO algorithms perform well in finding global optimum for high dimensional problem, but not so well in finding global optimum for low dimensional problems. As the problem in our situation, is only two-dimensional since the number of switching angles to compute for removing the third harmonic in a five-level PUC-MLI is only two. While there's no guarantee that GWO will identify global minima, it's possible that it will stick with local minima and calculate corresponding angles that don't totally eliminate the 3rd harmonic. To address this issue, a donor vector from a differential evolution technique is used, which adds randomness to the GWO technique and allows it to escape out of the local optimum and look in a new direction for the global optimum. Because the DE technique is based on complete random initialization, it outperforms to find the global optima, but it has a limitation in that it lacks a parameter that is directly related to algorithm convergence, so the speed of convergence is very slow and provides power oscillation around the global optima. As a result, the flaw in one approach is offset by other method. Therefore, a new algorithm called Improved grey wolf optimization and differential evolution (IGWO-DE) is proposed in this paper, which combines the GWO algorithm with a better convergence factor and the DE algorithm with a dynamic scaling factor with the help of a DE crossover operator. The initialization of a random vector of population size Np with dimension d under boundary conditions is the first step in the IGWO-DE method. Where d denotes the problem dimension or the number of variables in the problem, and this random vector is referred to as the target vector, which can be described as follows:

$$\vec{X}_{i,}^{t} = [x_{i,1}^{t},\ x_{i,2}^{t}, x_{i,3}^{t} \ldots\ldots, x_{i,d}^{t}\ ] \qquad (17)$$

Where $i\ \in \{1,2,3, \ldots \ldots N_p\}$, and t is the current value of iteration and each individual can be calculated as follows :

$$x_{i,j}^{1}\ =\ x_{lb} +\ rand(0,1) * (x_{ub} - x_{lb}) \qquad (18)$$

Where x_{ub}, x_{lb} are the upper bound and lower bound vectors with d individuals respectively. Similar to GWO, the three best solutions in IGWO-DE are saved as alpha ($\vec{X}_{\alpha}$), beta ($\vec{X}_{\beta}$), and delta ($\vec{X}_{\delta}$) solutions from the target vector. Following the saving of the solutions, the target vector is subjected to mutation in a manner similar to the DE technique. In our proposed algorithm, the donor vector $\vec{V}_{i}^{t}$ is generated from the target vector $\vec{X}_{i}^{t}$ using a DE/best/1 mutation strategy with a dynamic scaling factor F', which provides more randomness in the initial stages, preventing the algorithm from falling into a local optimum, while the value of F' decreases in the final stages, increasing the algorithm's convergence speed. So, the donor vector can be expressed as follows :

$$\vec{V}_i^t = \vec{X}_{alpha}^t + F' * (\vec{X}_{R1}^t - \vec{X}_{R2}^t) \qquad (19)$$

Where $\vec{X}_{alpha}^t$ is the alpha solution or best candidate solution as far and $\vec{X}_{R1}^t$, $\vec{X}_{R2}^t$ are the randomly selected solution from the target vector and F'can be expressed as follow :

$$F' = \frac{2}{\left(1 + e^{\left(k*\left(\frac{t}{tmax}\right)\right)}\right)} \; ; k \in [8,14] \qquad (20)$$

GWO's searching ability is primarily determined by the vectors $\vec{A}$ and $\vec{C}$, where $\vec{C}$ is a randomly generated vector ranging from 0 to 2, the wolves favour exploration if $\vec{C} > 1$ and exploitation if $\vec{C}< 1$, and $\vec{C}$ plays no role in GWO's convergence speed. Now, the only vector that is important in convergence is $\vec{A}$, but the value of $\vec{A}$ is determined by the convergence factor or a, and the value of a decreases linearly from 2 to 0 over the course of iteration. We need to modify the convergence factor to improve the speed of the algorithm. This paper proposed a new non linear convergence factor based on a sigmoid function that improves the speed of the algorithm, which can be expressed as follows. :

$$a = \frac{2}{\left(1 + e^{\left(k*\left(\frac{t}{t_{max}} - \frac{1}{2}\right)\right)}\right)} \; ; k \in [8,12] \qquad (21)$$

Using this improved convergence factor, the updated position of the wolves can be calculated using equations (6-12) on the basis of the position of the best wolves. Let us consider the i-th position vector of wolves in the t-th iteration as $\overrightarrow{W_i^t} = [w_{i,1}^t,\, w_{i,2}^t, w_{i,3}^t \dots\dots, w_{i,d}^t]$ which can be calculated using equation. Now these two vectors are combined using a binomial crossover operator to generate a position vector for next iteration. The new position vector can be described as follows:

$$X_{i,j}^{t+1} = \begin{cases} V_{i,j}^t \,, if\ rand(0,1) \le CR\ OR\ j = \delta \\ X_{i,j}^t, if\ rand(0,1) > CR\ AND\ j \neq \delta \end{cases} \qquad (22)$$

3.2 Implementation of Proposed Algorithm:

In order to minimize the THD defined as in equation, SHE technique is used in which some of the dominating harmonics must have been eliminated except the fundamental harmonic component of output waveform. In order to solve non-linear equations we have to define the fitness function and constraints.

$$THD = \frac{\sqrt{V_3^2 + V_5^2 + V_7^2 \dots\dots + V_\infty^2}}{V_1}$$

$$f = \frac{\sqrt{V_3^2 + V_5^2 + V_7^2 \dots \dots + V_{2S-1}^2}}{V_1}$$

But for 5 level MLI the value of S =2 so the fitness function and constraints can be defined as follows:

$$f(\alpha_1, \alpha_2) = \frac{\sqrt{V_3^2}}{V_1}$$

$$g_1 = \mathrm{Cos}(\alpha_1) + \cos(\alpha_2) \dots \dots \dots + \cos(\alpha_s) - M\frac{\pi}{2} = 0$$

$$g_2 = \cos(3\alpha_1) + \cos(3\alpha_2) \dots \dots + \cos(3\alpha_s) = 0$$

By using Deb's approach for non-linear constraint problem final objective function will be:

$$F(\alpha_1, \alpha_2) = \begin{cases} f, & if\ solution\ is\ feasible \\ f_{max} + g_1 + g_2, & otherwise \end{cases}$$

Where f_{max} is the worst fitness so far and the solution will be feasible only when it is satisfying all the constraints.

Flowchart of the IGWO-DE technique for the calculation of firing angles for SHE-PWM is shown in Figure 7. consists of several steps which can be described as follows:

Step 1: Initialise parameter including maximum iteration, population size, crossover rate, etc

Step 2: Generate a set of switching angles following condition ($0 < \alpha_1 < \alpha_2 < 90$)

Step 3: Calculate the fitness of each individual according to eqn.

Step 4: Determine the best three solutions as alpha, beta and delta solution by comparing the fitness value for each search agent.

Step 5: When all search agents fitness values are calculated, the position vector of the search agent for the next iteration is determined using the binomial crossover operator of differential evolution, which can be described as follows:

$$X_{i,j}^{t+1} = \begin{cases} V_{i,j}^t, if\ rand(0,1) \le CR \\ W_{i,j}^t, if\ rand(0,1) > CR \end{cases}$$

Where $V_{i,j}^t$ is the donor vector borrowed from the DE/best/1 mutation strategy described above in equation (19)(20), and $W_{i,j}^t$ it is the vector obtained using the position update strategy of the GWO technique with an improved convergence factor described in equation (6-12). (21)

Step 6: The IGWO-DE technique will terminate when the convergence criteria are met, i.e. when the number

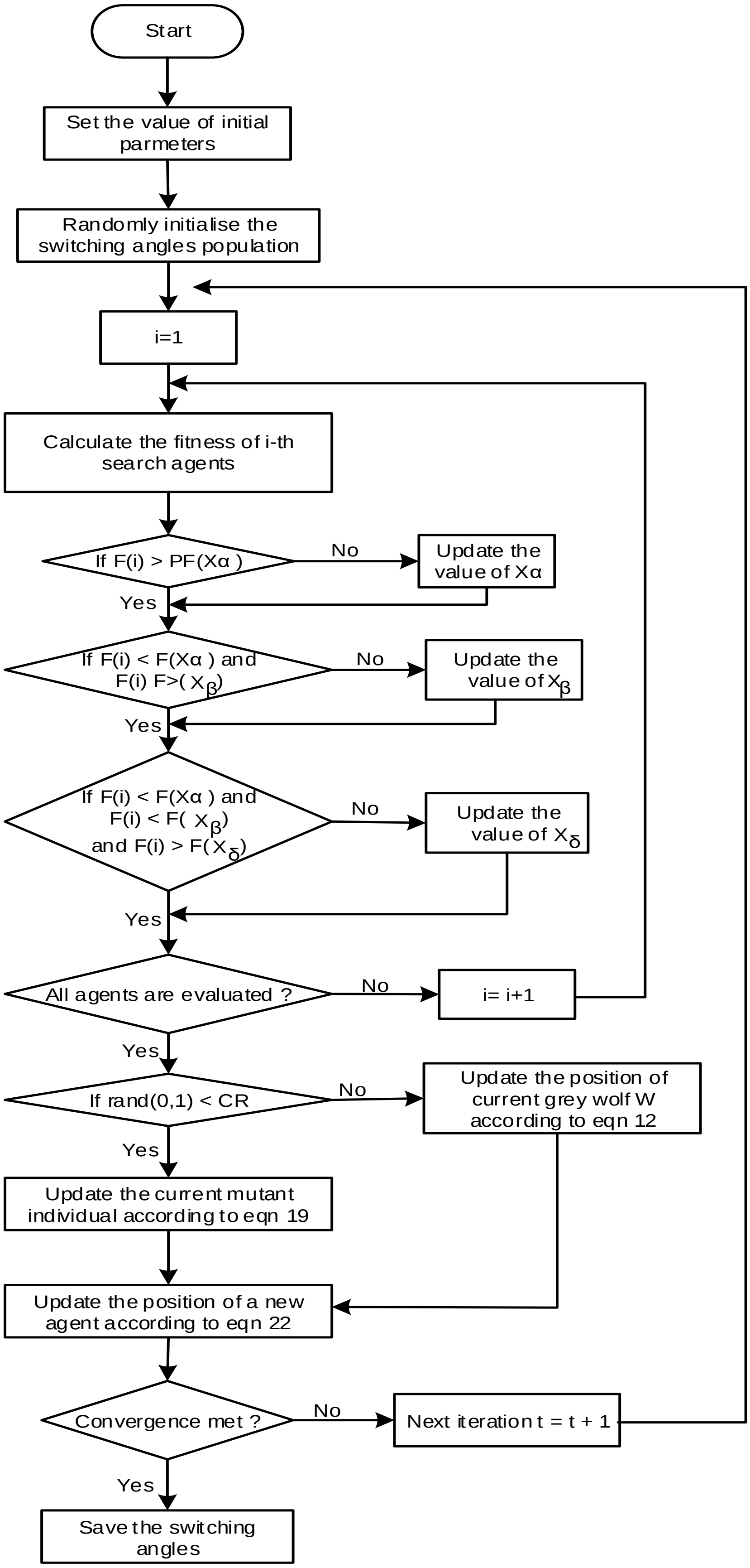

Figure 9: Flowchart of IGWO-DE

CHAPTER 4

4. Honey Badger Algorithm

4.1 Overview of Honey Badger Algorithm

Honey badger is a mammal with black and white fluffy fur often found in the semi-deserts and rainforests of Africa, Southwest Asia, and the Indian subcontinent — known for its fearless nature. This dog size (60 to 77 cm body length and 7 to 13 Kgs body weight) fearless forager preys sixty different species including the dangerous snakes. It is an intelligent animal able to use tools, and it loves honey. It prefers to stay solitary in self-dug holes, and meets the other badgers only to mate. There are 12 recognized honey badger subspecies. There is no specific breeding season for honey badgers as cubs are born throughout the year. Because of their courageous nature, it never hesitates attacking even much larger predators when it cannot escape (see Fig. 10). This animal also can easily climb on trees for reaching bird nests and beehives for food. A honey badger locates its prey by walking slowly continuously using smelling mouse skills. It starts to determine the approximate location of prey through digging and ultimately catching it. In a day, it can dig as many as fifty holes in a radius of forty kilometres more in foraging attempts. Honey badger likes honey, but it is not good in locating beehives. On the other hand, honey-guide (a bird) can locate the hives but cannot get honey. These phenomena lead a relationship between the two, where the bird leads the badger to beehives and helps it open hives using its long claws, then both enjoy the reward of teamwork

Figure 10: Honey Badger

Honey Badger Algorithm (HBA) imitates the foraging behaviour of honey badger. For locating food source, the honey badger either smells and digs or follows honeyguide bird. We call the first case as digging mode while the second as honey mode. In the prior mode, it uses its smelling ability to approximate prey location; when reaching there, it moves around the prey to select the appropriate place for digging and catching the prey. In latter mode, honey badger takes the guide of honeyguide bird to directly locate beehive.

4.2 Mathematical Modelling

This section introduces mathematical formulation of the proposed HBA algorithm. Theoretically, HBA is equipped with both exploration and exploitation phases, hence can be referred to as a global optimization algorithm. Mathematically, steps of the proposed HBA including population initialization, population evaluation, and updating parameters are detailed as the following. Here, population of candidate solutions in HBA is represented as:

$$\text{Population of candidate solutions} = \begin{bmatrix} x_{11} & x_{12} & x_{13} & \dots\dots\dots\dots & x_{1D} \\ x_{21} & x_{22} & x_{23} & \dots\dots\dots\dots & x_{2D} \\ x_{31} & x_{32} & x_{33} & \dots\dots\dots\dots & x_{3D} \\ \dots & \dots & \dots & \dots\dots\dots\dots & \dots \\ x_{n1} & x_{n2} & x_{n3} & \dots\dots\dots\dots & x_{nD} \end{bmatrix}$$

i-th position of honey badger, $x_i = [x_{i1} \; x_{i2} \; x_{i3} \dots\dots\dots\dots \; x_{iD}]$

Steps:

1. *Initialization phase:* Initialize the number of honey badgers (population size N) and their respective positions based on Eq. (23):
$$x_i = lb_i + r_1 * (ub_i - lb_i) \quad (23)$$
Where r_1 is a random number between 0 and 1, x_i is i-th honey badger position referring to a candidate solution in a population of N, while lb_i and ub_i are respectively lower and upper bounds of the search domain.
2. *Defining Intensity:* Intensity is related to concentration strength of the prey and distance between it and i-th honey badger. Ii is smell intensity of the prey; if the smell is high, the motion will be fast and vice versa, is given by Inverse Square Law is defined by Eq. (2).
$$\begin{gathered} I_i = r_2 * \left(\frac{S}{4\pi d_i^2}\right) \\ S = (x_i - x_{i+1})^2 \\ d_i = x_{prey} - x_i \end{gathered} \quad (24)$$
where S is source strength or concentration strength. In Eq. (24), di denotes distance between prey and the i-th badger.
3. *Update Density Factor:* The density factor (α) controls time-varying randomization to ensure smooth transition from exploration to exploitation. Update decreasing factor α that decreases with iterations to decrease randomization with time, using Eq. (25):
$$\alpha = C * \exp\left(\frac{-t}{t_{max}}\right) \quad (25)$$
Where t_{max} , *C* are the maximum number of iterations and constant which is greater than or equal to 1 usually taken as 2.
4. *Escaping from local optima:* This step and the two next steps are used to escape from local optima regions. In this context, the proposed algorithm uses a flag F which alters

search direction for availing high opportunities for agents to scan the search-space rigorously.

5. *Updating the agent position:* HBA position update process (X_{new}) is divided into two parts which are "digging phase" and "honey phase". Following is given better explanation:

a) *Digging Phase:* In digging phase, a honey badger performs action similar to Cardioid shape. The Cardioid motion can be simulated by Eq. (26):

$$X_{new} = X_{prey} + F\beta I X_{prey} + F r_3 \alpha d_i \{\cos(2\pi r_4) * \{1 - \cos(2\pi r_5)\}\} \quad (26)$$

where X_{prey} is position of the prey which is the best position found so far – global best position in other words. $\beta \geq 1$ (default = 6) is ability of the honey badger to get food. di is distance between prey and the ith honey badger, see Eq. (2). r3, r4, and r5 are three different random numbers between 0 and 1. *F* works as the flag that alters search direction, it is determined using Eqn. (27)

$$F = \left.\begin{cases} 1 & if\ r_6 \leq 0.5 \\ -1 & else \end{cases} \quad r_6\ is\ a\ random\ number\ between\ 0\ and\ 1\right\} (27)$$

In the digging phase, a honey badger heavily relies on smell intensity *I* of prey X_{prey} , distance between the badger and prey d_i, and time-varying search influence factor *α*. Moreover, during digging activity, a badger may receive any disturbance *F* which allows it to find even better prey location.

b) *Honey phase:* The case when a honey badger follows honey guide bird to reach beehive can be simulated as Eq. (28):

$$X_{new} = X_{prey} + F * \alpha * d_i * r_7 \quad (28)$$

Where X_{new} refer to the new position of honey badger, whereas X_{prey} is prey location, *F* and *α* are determined using Eqns. (27) and (25), respectively. From Eq. (28), it can be observed that a honey badger performs search close to prey location x prey found so far, based on distance information di . At this stage, the search is influenced by search behaviour varying by time (α). Moreover, a honey badger may find disturbance *F*.

4.3 Implementation of Honey Badger Algorithm

In order to minimize the THD defined as in equation, SHE technique is used in which some of the dominating harmonics must have been eliminated except the fundamental harmonic component of output waveform. In order to solve non-linear equations we have to define the fitness function and constraints.

$$THD = \frac{\sqrt{V_3^2 + V_5^2 + V_7^2 \ldots \ldots + V_\infty^2}}{V_1}$$

$$f = \frac{\sqrt{V_3^2 + V_5^2 + V_7^2 \dots \dots + V_{2S-1}^2}}{V_1}$$

But for 5 level MLI the value of S =2 so the fitness function and constraints can be defined as follows:

$$f(\alpha_1, \alpha_2) = \frac{\sqrt{V_3^2}}{V_1}$$

$$g_1 = \text{Cos}(\alpha_1) + \cos(\alpha_2) \dots \dots \dots + \cos(\alpha_s) - M\frac{\pi}{2} = 0$$

$$g_2 = \cos(3\alpha_1) + \cos(3\alpha_2) \dots \dots + \cos(3\alpha_s) = 0$$

By using Deb's approach for non-linear constraint problem final objective function will be:

$$F(\alpha_1, \alpha_2) = \begin{cases} f, & if\ solution\ is\ feasible \\ f_{max} + g_1 + g_2, & otherwise \end{cases}$$

Where f_{max} is the worst fitness so far and the solution will be feasible only when it is satisfying all the constraints.

Pseudocode of the HBA technique for the calculation of firing angles for SHE-PWM is shown below:

While $t \leq t_{max}$
    Update the decreasing factor $\propto$ using Eq. (25).
    For i = 1 to N do
        Calculate the intensity I_i using Eq. (24).
        If r < 0.5 then
            Update the position x_{new} using Eq. (26).
        Else
            Update the position x_{new} using Eq. (28)
        End if
        Evaluate new position and assign to f_{new}
        If $f_{new} \leq f_{prey}$ *then*
            Set $x_{prey} = x_{new}$ and $f_{prey} = f_{new}$
        End if
    end for
end while Stop criteria satisfied
Return x_{prey}

Figure 11: Pseudocode of HBA

CHAPTER 5

5. RESULTS AND DISCUSSION

5.1 Simulation Results of IGWO-DE Algorithm:

The PUC-5 multilevel inverter is modelled using MATLAB/Simulink software. The first step in using SHE-PWM is to derive a non-linear or transcendental equation from the fourier expansion. In this study, a novel hybrid approach known as IGWO-DE is used to solve these nonlinear equations. These switching angles were used to turn ON or turn OFF the PUC-5 inverter's switches.

The simulation results for modulation indices of 0.75, 0.85, and 0.90 are shown in the figures, along with their output waveforms and harmonic spectra. For each MI there are five output voltage levels: 100V, 50V, 0V, -50V, and -100V, where the Dc source voltage is 100V and the nominal output frequency is assumed to be 50 Hz.

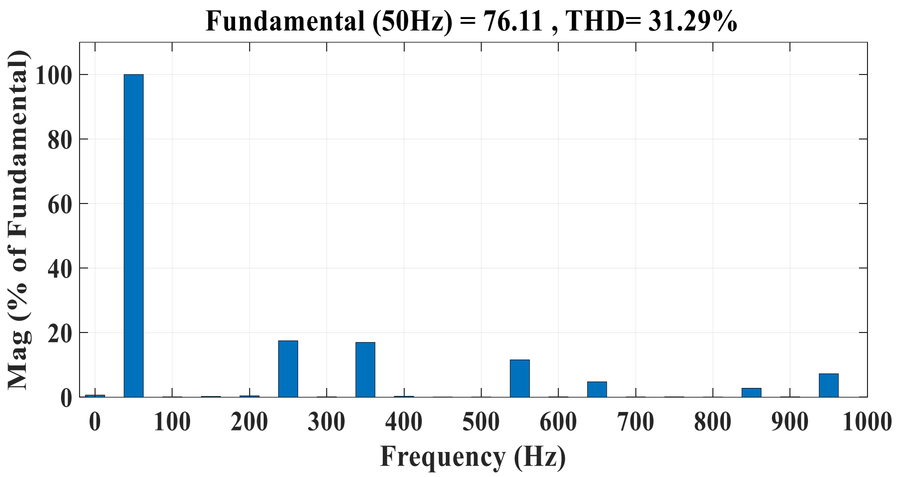

(a)

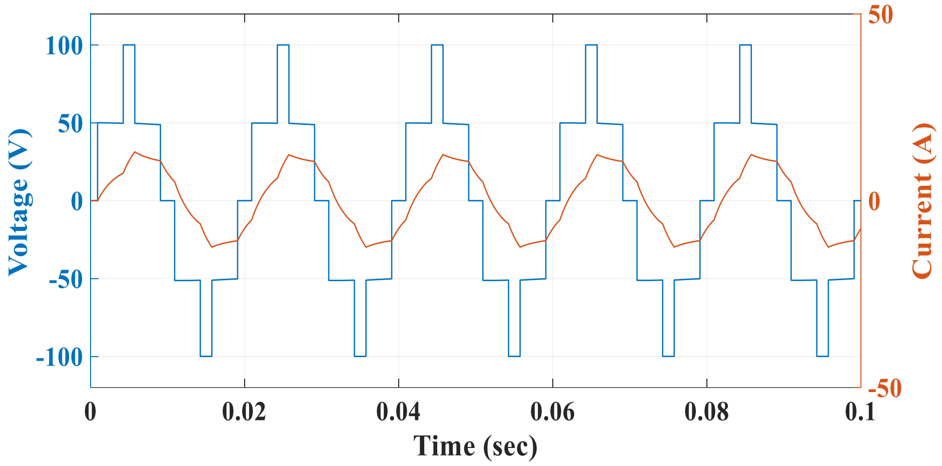

(b)

Figure 12: (a) Harmonic spectrum for M=0.75 (b): Output waveform of PUC-5 multilevel inverter for M =0.75

The harmonic spectrum of the output voltage waveform is shown in Figure 12(a), and the total harmonic distortion for a 5-level PUC inverter with a modulation index of 0.75 is 31.29 percent.

We used the proposed algorithm to completely remove the third harmonic, and the simulation result confirms that the third harmonic has been completely removed from the harmonic spectrum. And, as shown in Figure 12(b), all five levels of PUC-5 MLI are completely visible.

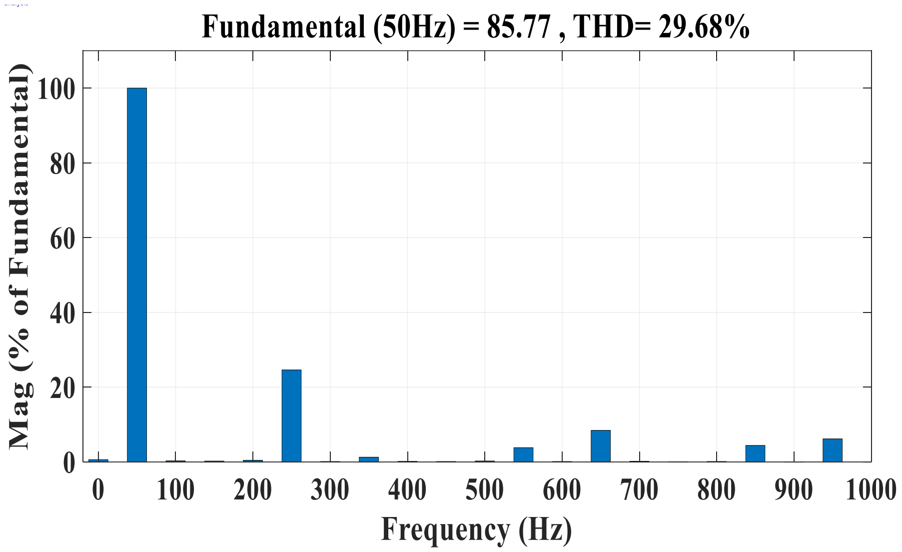

(a)

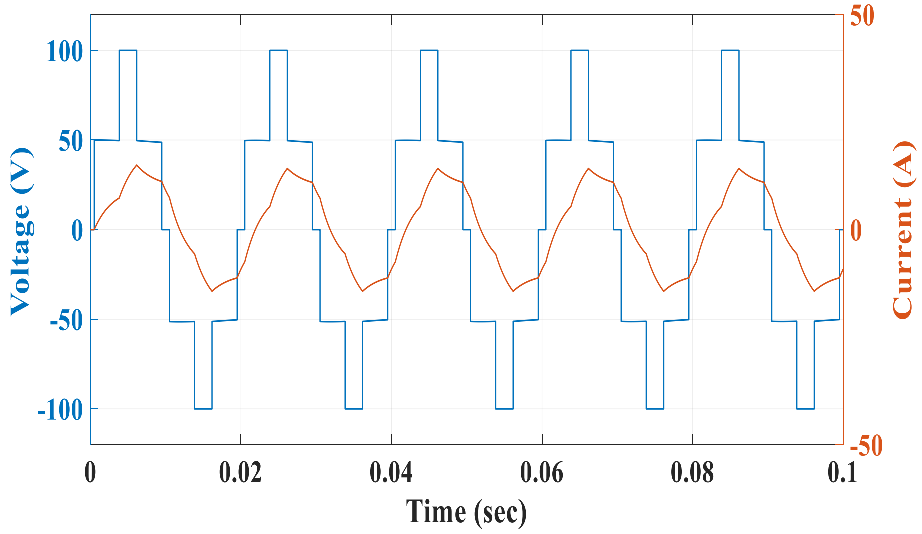

(b)

Figure 13: (a) Harmonic spectrum for M=0.85 (b): Output waveform of PUC-5 multilevel inverter for M =0.85

According to Figure 13(a), the total harmonic distortion for a 5-level PUC inverter with a modulation index of 0.85 is 29.68 percent. As shown in Figure 13(b), the output waveform contains all five levels, and it can be seen that the 0th level decreases as the MI and THD increase.

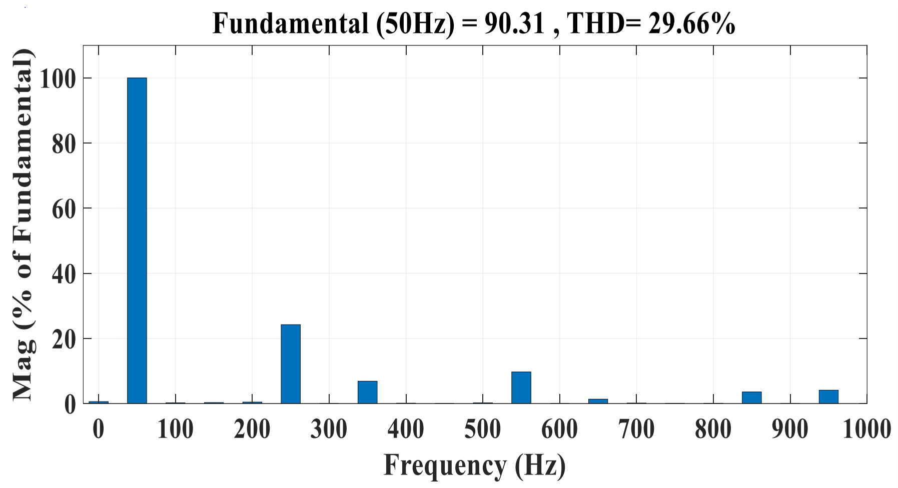

(a)

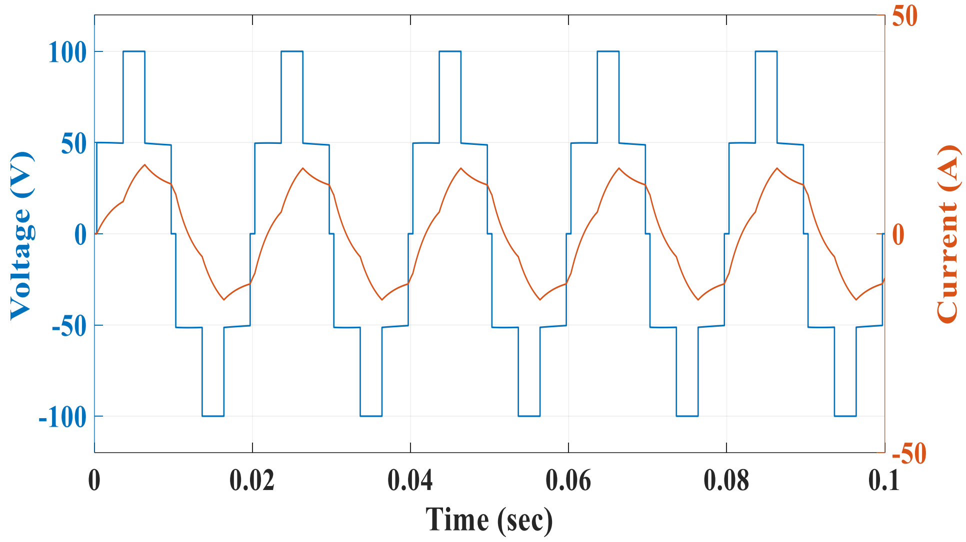

(b)

Figure 14: (a) Harmonic spectrum for M=0.90 (b): Output waveform of PUC-5 multilevel inverter for M =0.90

Figure 14 shows that the total harmonic distortion in the output voltage waveform is 29.66 percent at 0.90 MI (a). Furthermore, the harmonic spectrum's third harmonic has been completely eliminated. All of the above simulation results show that our proposed algorithm is effective at finding switching angles to remove the third harmonic and reduce THD. The above results also show that as the MI increases, the THD decreases, and the lowest THD so far is at MI of 0.9.

5.2 Comparison of IGWO-DE Algorithm:

Table 2: Comparison presence of order of harmonics for different algorithms

Modulation Index	0.75			0.85		
Order Of Harmonics	THIRD (%)	FIFTH (%)	SEVENTH (%)	THIRD (%)	FIFTH (%)	SEVENTH (%)
GWO	1.53	16.68	17.62	1.33	25.29	1.5
DE	0.87	16.3	18.08	1.93	16.06	18.36
IGWO-DE	**0.78**	**16.7**	**17.81**	**0.2**	**24.74**	**0.28**

Table 3: Comparison of THD for different algorithms

	THD (%)	
Modulation Index	0.75	0.85
GWO	31.74	30.2
DE	31.41	29.99
IGWO-DE	**31.29**	**29.68**

According to Table 2, the content of third harmonics present at a modulation index of 0.75 in GWO is 1.53 percent, 0.87 percent in DE, and 0.78 percent in the proposed algorithm IGWO-DE. At a modulation index of 0.85, GWO is 1.33 percent, DE is 1.93 percent, but IGWO-DE outperforms all algorithms. The third harmonics content was almost completely removed, with only 0.2 percent remaining.

5.3 Simulation Results of HBA:

MATLAB/Simulink software is used to model the PUC-5 multilevel inverter. The first step in employing SHE-PWM is to deduce a non-linear or transcendental equation from the fourier expansion. To solve these nonlinear equations, a novel hybrid approach known as HBA is used in this study. These switching angles were used to enable or disable the PUC-5 inverter's switches.

Figures show the simulation results for modulation indices of 0.75, 0.85, and 0.90, as well as their harmonic spectra. There are five output voltage levels for each MI: 100V, 50V, 0V, -50V, and -100V, where the Dc source voltage is 100V and the nominal output frequency is 50 Hz.

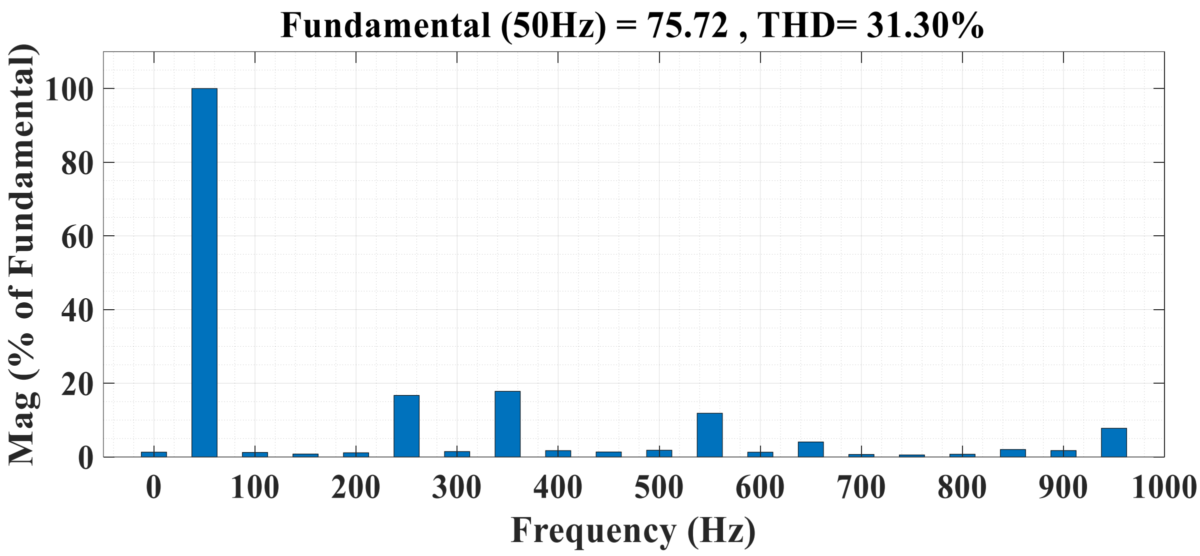

Figure 15: Harmonic spectrum for M=0.75

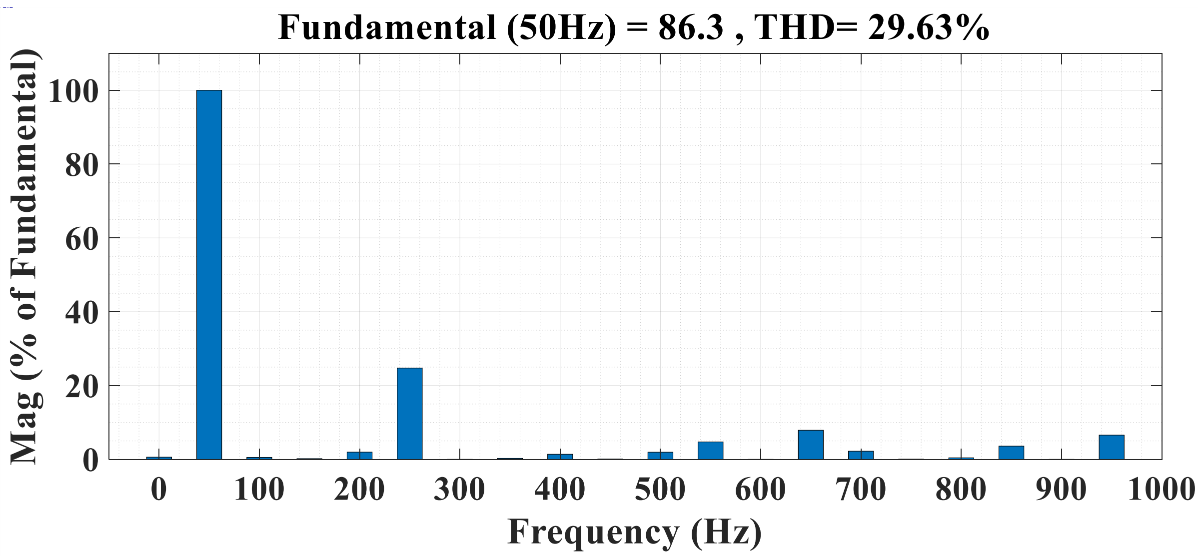

Figure 16: Harmonic spectrum for M=0.85

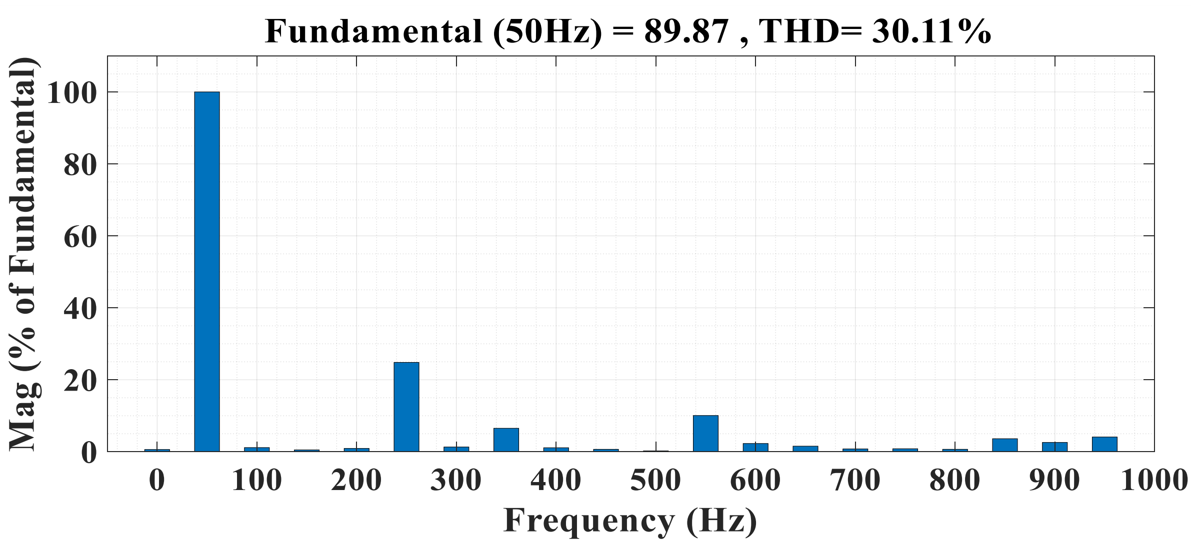

Figure 17: Harmonic spectrum for M=0.90

5.4 Experimental Results

To validate the simulation results, the proposed algorithm is implemented on a prototype and experimental results for a PUC-5 MLI are obtained. The prototype is made up of six MOSFET switches, a 200V dc source, and a capacitor. The switching angles discovered in MATLAB by employing the proposed algorithm are directly programmed into the DSP (Digital signal processor) board. It is used to generate the desired pulses for MOSFETS switching. A Rheostat with a variable load range of 0-100 ohm is also used.

The experimental results are taken for three different MI values, which are 0.75, 0.85, and 0.9, just like the simulation results. The output voltage current waveform and their corresponding harmonic spectra at a load of 100 ohm observed using a DSO. This shows that all five levels are visible, namely 0V, 100V, 200V, -100V, -200V, with the amount of each level varying in each case, and the 0th level decreasing as the value of MI increases, with the maximum value of current found to be 2A.

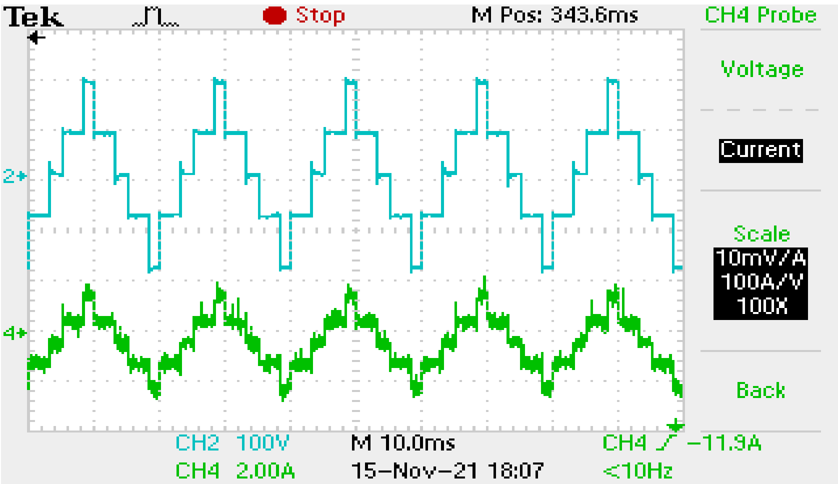

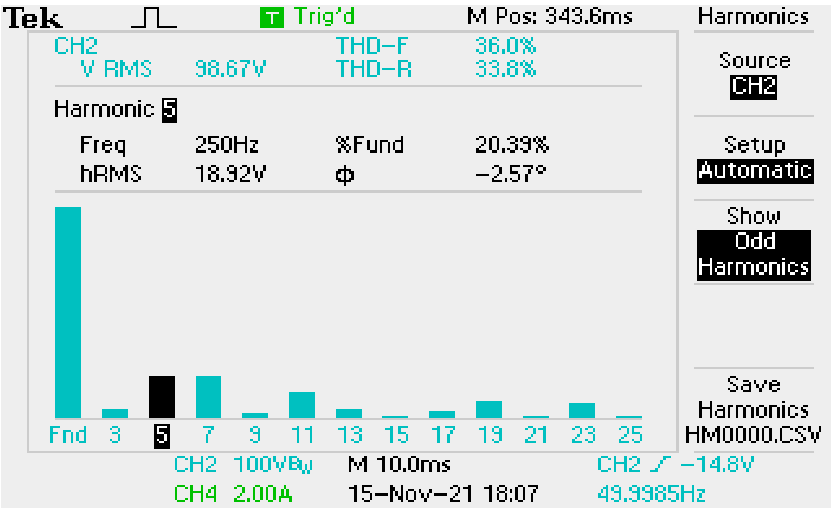

(a)

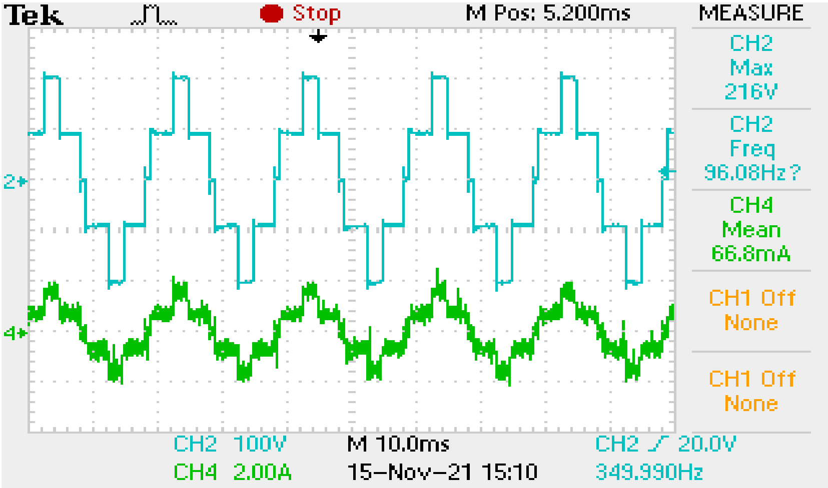
Tek
Stop
M Pos: 5.200ms
MEASURE
CH2
Max
216V
CH2
Freq
96.08Hz?
CH4
Mean
66.8mA
CH1 Off
None
CH1 Off
None
CH2 100V
CH4 2.00A
M 10.0ms
15–Nov–21 15:10
CH2 ⁄ 20.0V
349.990Hz

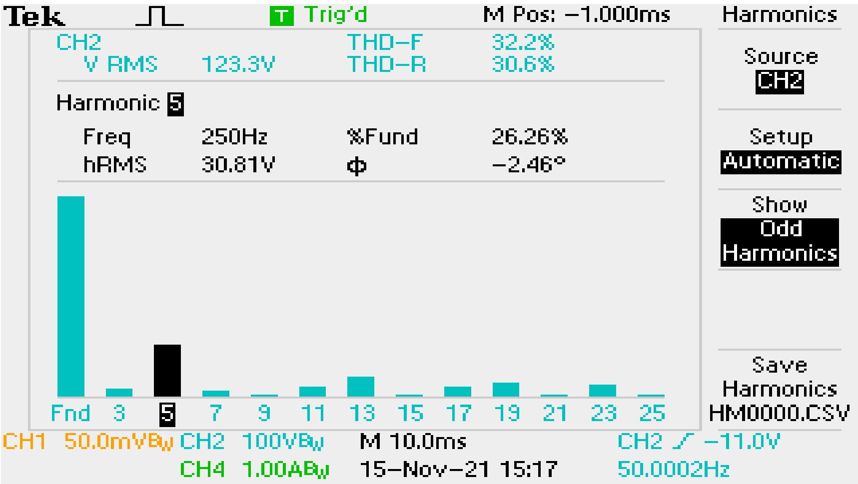
Tek
Trig'd
M Pos: –1.000ms
Harmonics
CH2
V RMS 123.3V
THD–F 32.2%
THD–R 30.6%
Harmonic 5
Freq 250Hz
%Fund 26.26%
hRMS 30.81V
φ –2.46°
Source
CH2
Setup
Automatic
Show
Odd
Harmonics
Save
Harmonics
HM0000.CSV
Fnd 3 5 7 9 11 13 15 17 19 21 23 25
CH1 50.0mVBW
CH2 100VBW
CH4 1.00ABW
M 10.0ms
15–Nov–21 15:17
CH2 ⁄ –11.0V
50.0002Hz

(b)

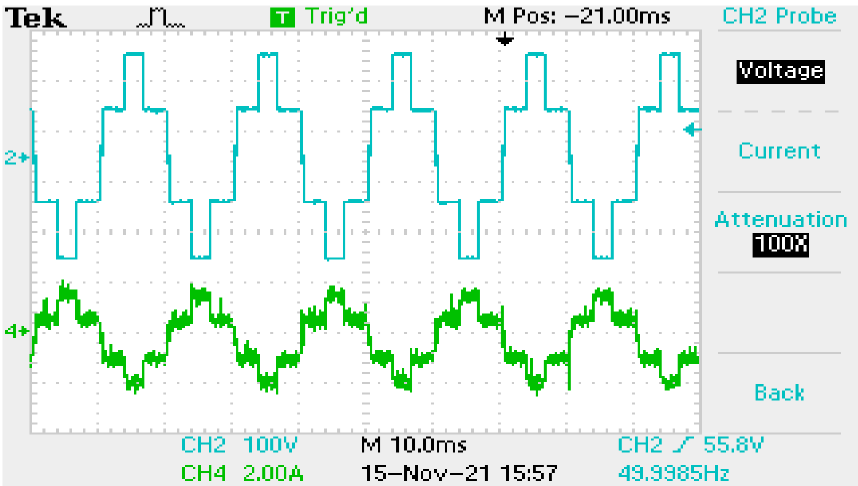
Tek
Trig'd
M Pos: –21.00ms
CH2 Probe
Voltage
Current
Attenuation
100X
Back
CH2 100V
CH4 2.00A
M 10.0ms
15–Nov–21 15:57
CH2 ⁄ 55.8V
49.9985Hz

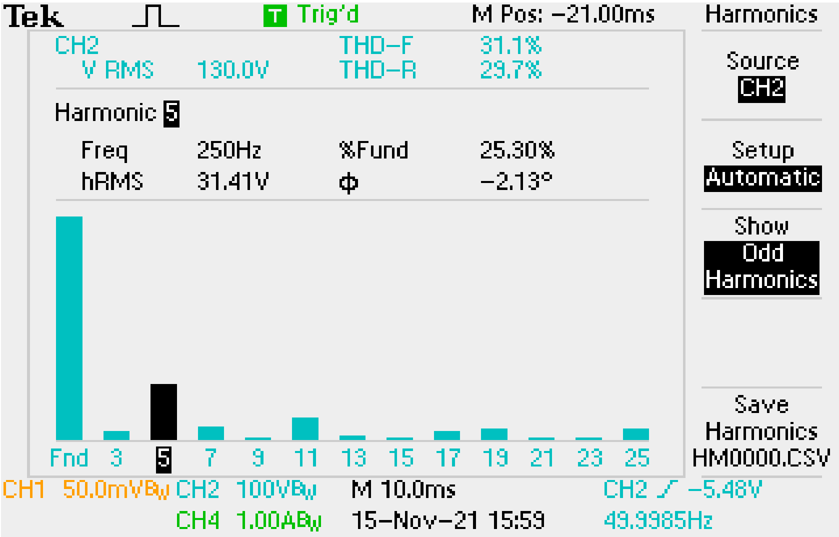

(c)

Figure 18: Output Waveforms of PUC-5 MLI with their corresponding harmonic spectrum (a) for M = 0.75 at a load of 100 ohm (b) for M = 0.85 at a load of 100 ohm (c) for M = 0.90 at a load of 100 ohm.

Figure 17 shows that the third harmonic is almost eliminated in all three different values of MI, which validates the simulation result. THD is found to be 33.8 percent, 30.6 percent, and 29.7 percent at MIs of 0.75, 0.85, and 0.90, respectively. As we can see, the THD decreases as the MI increases, and the values of THD are also very close to the values of the simulation result. The minimum THD is found in all three cases at the MI of 0.90, so the output voltage and current for dynamic load change are also shown in Figure12.

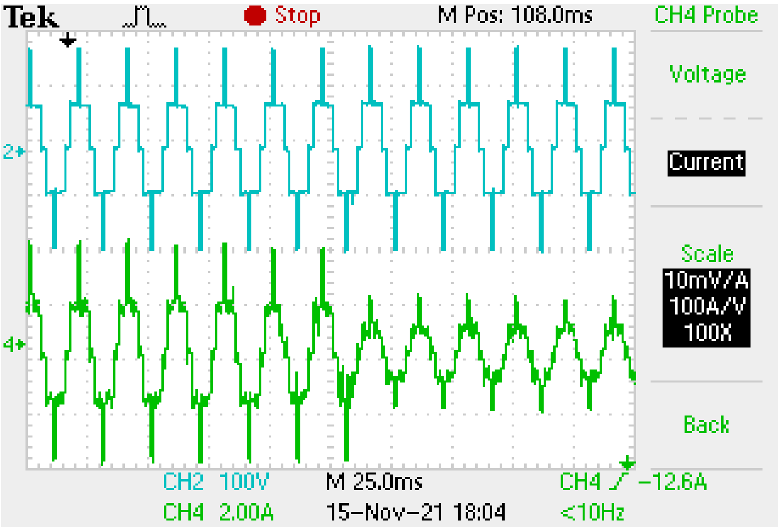

(a)

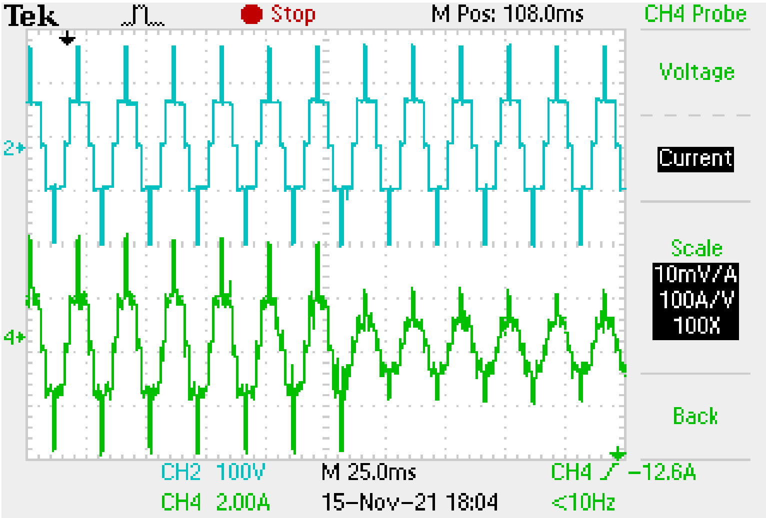

(b)

Figure 19: Output Waveforms of PUC-5 MLI at MI = 0.90 (a) load is increased from 50ohm to 100ohm (b) load is decreased from 100ohm to 50ohm.

Figure 18 shows that the output voltage is unaffected by the change in load; only the current is altered. When the load resistance is raised, the peak current in case 1 drops from 4A to 2A, as illustrated in Figure 18. (a). Similarly, as the load drops from 100 to 50 ohm, the current is increased from 2A to 4A. It may be deduced from Figure 18 that the current is inversely proportional to the load. Due to the use of a DSP board for switching, voltage stress developed across the switches, as seen in Figure 19.

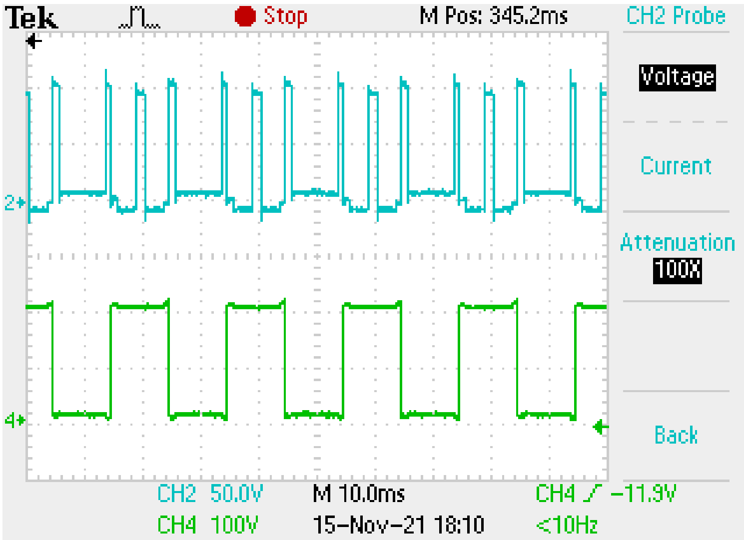

(a)

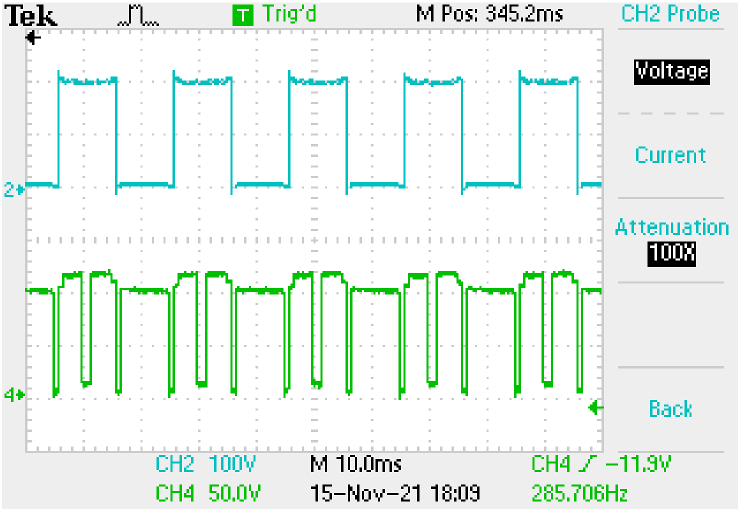

(b)

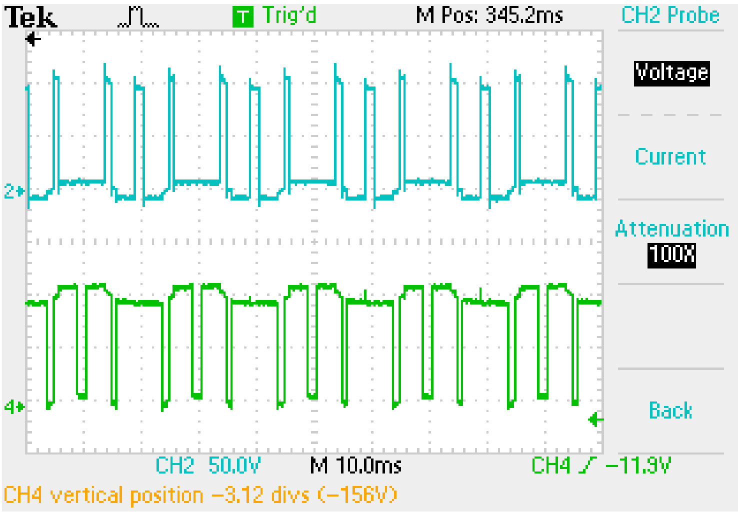

(c)

Figure 20: Voltage stresses along the switches (a) S1 & S2 (b) S3 & S4 (c) S5 & S6.

CHAPTER 6

6. CONCLUSION AND REFERENCE

6.1 Conclusion

This paper presents the IGWO-DE technique to eliminate the low order harmonic from the output waveform of a multilevel inverter for minimizing the THD. MATLAB-SIMULINK was used to evaluate the proposed algorithm in order to eliminate the 3rd harmonic from the output waveform of a 5 level PUC-MLI for different values of modulation indices. The simulation results also showed that it is capable of determining the best switching angles for a multilevel inverter. Furthermore, the suggested algorithm may be applied to all levels of symmetrical/asymmetrical inverters and has a variety of other applications, such as locating a global-maxima in partial shadowing conditions for a renewable energy system.

6.2 References

1. C. Dhanamjayulu, S. Padmanaban, V. K. Ramachandaramurthy, J. B. Holm-Nielsen, and F. Blaabjerg, "Design and Implementation of Multilevel Inverters for Electric Vehicles," *IEEE Access*, vol. 9, no. January, pp. 317–338, 2021, doi: 10.1109/ACCESS.2020.3046493.
2. L. M. Tolbert, F. Z. Peng, and T. G. Habetler, "Multilevel converters for large electric drives," *IEEE Trans. Ind. Appl.*, vol. 35, no. 1, pp. 36–44, 1999, doi: 10.1109/28.740843.
3. E. Ceuca and G. Corsiuc, "The Smart City - Integrated green energy system," *Proc. Int. Spring Semin. Electron. Technol.*, vol. 2015-Septe, no. December 1918, pp. 390–395, 2015, doi: 10.1109/ISSE.2015.7248028.
4. S. Choudhury, M. Bajaj, T. Dash, S. Kamel, and F. Jurado, "Multilevel inverter: A survey on classical and advanced topologies, control schemes, applications to power system and future prospects," *Energies*, vol. 14, no. 18, 2021, doi: 10.3390/en14185773.
5. P. Ponnusamy *et al.*, "A new multilevel inverter topology with reduced power components for domestic solar PV applications," *IEEE Access*, vol. 8, pp. 187483–187497, 2020, doi: 10.1109/ACCESS.2020.3030721.
6. E. H. E. Aboadla, S. Khan, M. H. Habaebi, T. Gunawan, B. A. Hamidah, and M. Tohtayong, "Selective Harmonics Elimination technique in single phase unipolar H-bridge inverter," *Proc. - 14th IEEE Student Conf. Res. Dev. Adv. Technol. Humanit. SCOReD 2016*, no. December, 2017, doi: 10.1109/SCORED.2016.7810057.
7. M. S. A. Dahidah, G. Konstantinou, and V. G. Agelidis, "A Review of Multilevel Selective Harmonic Elimination PWM: Formulations, Solving Algorithms, Implementation and Applications," *IEEE Trans. Power Electron.*, vol. 30, no. 8, pp. 4091–4106, 2015, doi: 10.1109/TPEL.2014.2355226.
8. W. A. Halim, T. N. A. Tengku Azam, K. Applasamy, and A. Jidin, "Selective harmonic elimination based on newton-raphson method for cascaded H-bridge multilevel inverter," *Int. J. Power Electron. Drive Syst.*, vol. 8, no. 3, pp. 1193–1202, 2017, doi: 10.11591/ijpeds.v8i3.pp1193-1202.
9. H. Wang and Q. Wang, "A new Gauss–Newton-like method for nonlinear equations," *Turkish J. Math.*, vol. 45, no. 1, pp. 264–280, 2021, doi: 10.3906/MAT-1912-68.
10. C. Buccellay, C. Cecatiy, and M. G. Cimoroni, "Investigation about numerical methods for Selective Harmonics Elimination in cascaded multilevel inverters," *Electr. Syst. Aircraft, Railw. Sh. Propulsion, ESARS*, 2012, doi: 10.1109/ESARS.2012.6387437.
11. M. K. T. Kirti and V. Goyal, "Implementation of Algebraic Method Based Selective Harmonic

Elimination of Multilevel Inverter Using Artificial Neural Networks," *Pdfs.Semanticscholar.Org*, vol. 9, no. 4, pp. 467–482, 2017, [Online]. Available: https://pdfs.semanticscholar.org/69a1/84f780aef1b62e21d62e3ca74ae91265f17d.pdf.
12. K. H. Yang, Z. B. Yuan, W. Wei, R. Y. Yuan, and W. S. Yu, "Solve the selective harmonic elimination problem with groebner bases theory," *Chinese Control Conf. CCC*, vol. 2015-Septe, no. 2, pp. 7910–7915, 2015, doi: 10.1109/ChiCC.2015.7260897.
13. K. Yang, L. Chen, J. Zhang, J. Hao, and W. Yu, "Parallel resultant elimination algorithm to solve the selective harmonic elimination problem," *IET Power Electron.*, vol. 9, no. 1, pp. 71–80, 2016, doi: 10.1049/iet-pel.2015.0070.
14. J. N. Chiasson, L. M. Tolbert, K. J. McKenzie, and Z. Du, "Elimination of Harmonics in a Multilevel Converter Using the Theory of Symmetric Polynomials and Resultants," *IEEE Trans. Control Syst. Technol.*, vol. 13, no. 2, pp. 216–223, 2005, doi: 10.1109/TCST.2004.839556.
15. J. N. Chiasson, L. M. Tolbert, Z. Du, and K. J. McKenzie, "The use of power sums to solve the harmonic elimination equations for multilevel converters," *EPE J. (European Power Electron. Drives Journal)*, vol. 15, no. 1, pp. 19–27, 2005, doi: 10.1080/09398368.2005.11463578.
16. M. A. Memon, M. D. Siddique, S. Mekhilef, and S. Member, "based Selective Harmonic Elimination in a Cascaded H-Bridge Multilevel Inverter."
17. E. Bektas and H. Karaca, "GA based selective harmonic elimination for multilevel inverter with reduced number of switches: An experimental study," *Elektron. ir Elektrotechnika*, vol. 25, no. 3, pp. 10–17, 2019, doi: 10.5755/j01.eie.25.3.23670.
18. Z. Salam, A. Majed, and A. M. Amjad, "Design and implementation of 15-level cascaded multi-level voltage source inverter with harmonics elimination pulse-width modulation using differential evolution method," *IET Power Electron.*, vol. 8, no. 9, pp. 1740–1748, 2015, doi: 10.1049/iet-pel.2014.0482.
19. A. Kavousi, B. Vahidi, R. Salehi, M. K. Bakhshizadeh, N. Farokhnia, and S. H. Fathi, "Application of the bee algorithm for selective harmonic elimination strategy in multilevel inverters," *IEEE Trans. Power Electron.*, vol. 27, no. 4, pp. 1689–1696, 2012, doi: 10.1109/TPEL.2011.2166124.
20. M. H. Etesami, N. Farokhnia, and S. Hamid Fathi, "Colonial competitive algorithm development toward harmonic minimization in multilevel inverters," *IEEE Trans. Ind. Informatics*, vol. 11, no. 2, pp. 459–466, 2015, doi: 10.1109/TII.2015.2402615.
21. M. Wetter and J. Wright, "Comparison of a Generalized Pattern Search and a Genetic Algorithm Optimization Method," *Ibpsa*, pp. 1401–1408, 2003.
22. P. Kala and S. Arora, "Implementation of PSO based selective harmonic elimination technique in multilevel inverters," *2018 2nd IEEE Int. Conf. Power Electron. Intell. Control Energy Syst. ICPEICES 2018*, pp. 605–610, 2018, doi: 10.1109/ICPEICES.2018.8897309.
23. P. Q. Dzung, N. T. Tien, N. DInh Tuyen, and H. H. Lee, "Selective harmonic elimination for cascaded multilevel inverters using Grey Wolf Optimizer algorithm," *9th Int. Conf. Power Electron. - ECCE Asia "Green World with Power Electron. ICPE 2015-ECCE Asia*, pp. 2776–2781, 2015, doi: 10.1109/ICPE.2015.7168164.
24. A. Routray, R. kumar Singh, and R. Mahanty, "Harmonic Minimization in Three-Phase Hybrid Cascaded Multilevel Inverter Using Modified Particle Swarm Optimization," *IEEE Trans. Ind. Informatics*, vol. PP, no. c, p. 1, 2018, doi: 10.1109/TII.2018.2883050.
25. M. S. A. Dahidah and V. G. Agelidis, "A hybrid genetic algorithm for selective harmonic elimination control of a multilevel inverter with non-equal DC sources," *Proc. Int. Conf. Power Electron. Drive Syst.*, vol. 2, pp. 1205–1210, 2005, doi: 10.1109/peds.2005.1619871.
26. M. Pakdel and S. Jalilzadeh, "A New Family of Multilevel Grid Connected Inverters Based on Packed U Cell Topology," *Sci. Rep.*, vol. 7, no. 1, pp. 1–9, 2017, doi: 10.1038/s41598-017-12806-5.
27. A. Gaikwad and P. A. Arbune, "Study of cascaded H-Bridge multilevel inverter," *Int. Conf. Autom. Control Dyn. Optim. Tech. ICACDOT 2016*, pp. 179–182, 2017, doi:

10.1109/ICACDOT.2016.7877574.

28. A. Shukla, A. Ghosh, and A. Joshi, “Flying capacitor multilevel inverter and its applications in series compensation of transmission lines,” *2004 IEEE Power Eng. Soc. Gen. Meet.*, vol. 2, pp. 1453–1458, 2004, doi: 10.1109/pes.2004.1373109.
29. J. Rodriguez, S. Bernet, P. K. Steimer, and I. E. Lizama, “A survey on neutral-point-clamped inverters,” *IEEE Trans. Ind. Electron.*, vol. 57, no. 7, pp. 2219–2230, 2010, doi: 10.1109/TIE.2009.2032430.
30. N. Manoj Kumar, C. Chellamuthu, and K. K. Prabhakaran, “Simulation and implementation of diode clamped multilevel inverter fed induction motor,” *Int. J. Appl. Eng. Res.*, vol. 9, no. 21, pp. 11433–11451, 2014.
31. H. Vahedi, P. A. Labbé, and K. Al-Haddad, “Sensor-Less Five-Level Packed U-Cell (PUC5) Inverter Operating in Stand-Alone and Grid-Connected Modes,” *IEEE Trans. Ind. Informatics*, vol. 12, no. 1, pp. 361–370, 2016, doi: 10.1109/TII.2015.2491260.
32. H. Vahedi, M. Sharifzadeh, and K. Al-Haddad, “Topology and control analysis of single-DC-source five-level packed U-cell inverter (PUC5),” *Proc. IECON 2017 - 43rd Annu. Conf. IEEE Ind. Electron. Soc.*, vol. 2017-Janua, pp. 8691–8696, 2017, doi: 10.1109/IECON.2017.8217527.
33. F. Gonzalez-rodriguez, R. Portillo, and E. Zafra-ratia, “Real-Time Selective Harmonic Mitigation Technique for Power Converters Based on the Exchange Market Algorithm,” doi: 10.3390/en13071659.
34. S. Mirjalili, S. M. Mirjalili, and A. Lewis, “Grey Wolf Optimizer,” *Adv. Eng. Softw.*, vol. 69, pp. 46–61, 2014, doi: 10.1016/j.advengsoft.2013.12.007.
35. R. Storn, “Differential Evolution – A Simple and Efficient Heuristic for Global Optimization over Continuous Spaces,” pp. 341–359, 1997.